DEPARTMENT OF THE INTERIOR

U.S. GEOLOGICAL SURVEY

Differential displacements and spectra for the April 26, 1981 Westmorland and the January 26, 1986 Hollister earthquakes

by

G. N. Bycroft and P. N. Mork[1]

Open-File Report No. 87-62

This report is preliminary and has not been reviewed for conformity with Geological Survey editorial standards and nomenclature.

1. Menlo Park, California

Differential Displacements and Spectra for the April 26, 1981 Westmorland and the January 26, 1986 Hollister Earthquakes

G. N. Bycroft and P. N. Mork

Abstract

Differential ground motion, under the base of a structure, imposes direct strain on the structure in addition to the strains caused by inertial loading. In order to assess the importance of these differential strains, differential arrays of digital accelerometers with pre-event memory were installed at El Centro and Hollister, California. These arrays produced useful data for the 1979 El Centro, the 1984 Morgan Hill, the 1981 Westmorland, and the 1986 Hollister earthquakes. This report gives differential displacements and spectra for the 1981 Westmorland and the 1986 Hollister earthquakes. In certain circumstances the differential strains are significant.

Introduction

Aseismic design generally has assumed that all points on the ground move in unison with the free-field motion over a region that is larger than the foundation of the structure. This assumption is based on the notion that seismic waves are substantially propagated substantially in high-wave-velocity basement rock and transmitted vertically to the region of interest through lower velocity layers. However, surface waves propagating horizontally through surface layers may have wavelengths along the surface of approximately the dimensions of a large structure (Trifunac, 1972; Wong and Trifunac, 1974; Bycroft, 1980). Further, differential ground motion may be caused by local inhomogeneity. The foundation of the structure would then undergo differential motions that would cause additional strains to be superimposed on those due to inertial loading. Thus, for example, adjacent bridge piers would move relative to each other and cause stresses in the piers and the bridge decking. Structures built on spread footings, dams and pipelines would be similarly affected.

To study such motion, differential ground motions must be measured. Methods of utilizing this information in aseismic design should be developed. Arrays of seismometers have been installed at El Centro and Hollister, California. These arrays are discussed in Bycroft (1982, 1983). Figure 1 shows the configuration of the Hollister array. The El Centro array runs north and south at distances of 0, 60, 180, 420, 700, and 1000 feet.

Differential Displacments

The processing of accelerograms to give displacements has long been a problem due to the double integrations of base-line error, long-period noise quantification errors, and problems related to the mechanics of film transportation. The original processing was directed towards digitized film records and was developed initially at the California Institute of Technology. Many changes have been made at the U.S.G.S. resulting in a present form known as AGRAM (Converse, 1984). This program has many options available depending on the judgement of the user for his particular application or data. The processing includes instrument corrections, base line corrections and high pass filtering to eliminate long period noise and quantification errors.

The program uses a Butterworth filter on the velocity running both ways to correct for phase. This, however, together with an inadequate base-line correction, leads to a finite initial velocity which, when integrated, leads to an initial rise or fall in the displacement, increasing with the width of the high pass filter. Displacements themselves are of no interest because only the difference of displacements occur in structural equations. This difference will eliminate those real long period seismic signals whose wavelengths are large compared to the spacing of the stations. Consequently, only differences of displacements will be considered. The processing adopted was to find a system which, for a series of filter widths would give reasonably similar differences with a minimum of rise or fall in the beginning of the calculated differences. This process is not necessarily the same for different sets of records.

Differential Spectra

In order to examine the significance of a structure being subjected to differential strain loading, in addition to the inertial loading, a simple model, which is affected by both these loadings was investigated. Figure 2 shows this structure as a simple one span bridge type of structure with two vertical piers connected by a deck. Transverse horizontal ground motions are applied to this structure so that shear stresses are developed in the three components. The masses are lumped together where the deck joins the piers. The masses are equal to m, the stiffness of the piers is k_1 and the stiffness of the deck is k_2. Different horizontal displacements $y_1(t)$ and $y_2(t)$ are applied to the base of each pier. A response spectrum R was calculated. This response spectrum is defined as the ratio of the maximum strain in pier 1 when the displacement inputs are $y_1(t)$ and $y_2(t)$ to that of the maximum strain in pier 1 when $y_1(t) = y_2(t)$. This ratio R is then a suitable measure of the effect of the addition of differential strain to the inertial loading. It is readily shown that

(1) $$R = \frac{A}{B}$$

where

(2) $$A = \frac{\text{Max}}{2} \int_0^t C \, d\tau$$

where Max means the maximum value of the integral during the length of the input and where

(3) $$C = \frac{e^{-\lambda\omega_1(t-\tau)}\{\ddot{y}_1(\tau)+\ddot{y}_2(\tau)\}\sin\omega_1(t-\tau)}{\omega_1} + \frac{e^{-\lambda\sqrt{\omega_1^2+2\omega_2^2}(t-\tau)}[\ddot{y}_1(\tau)-\ddot{y}_2(\tau)+2\omega_2^2\{y_1(\tau)-y_2(\tau)\}]\sin[\sqrt{\omega_1^2+2\omega_2^2}(t-\tau)]}{\sqrt{\omega_1^2+2\omega_2^2}}$$

(4) $$B = \text{Max} \int_0^t \frac{e^{-\lambda\omega_1(t-\tau)}\ddot{y}_1(\tau)[\sin\omega_1(t-\tau)]}{\omega_1} d\tau$$

where

(5) $\omega_1 = \sqrt{\frac{k_1}{m}}$

(6) $\omega_2 = \sqrt{\frac{k_2}{m}}$

(7) λ = modal damping factor

Similar equations apply to the longitudinal horizontal motions.

These spectra are for a simple two degree of freedom structure and are relevant to situations where the two stations are close. A multi-degree-of-freedom spectra is being developed that is more relevant to stations farther apart.

1986 Hollister Records

The Hollister Differential Array stations 1, 3, 5, 6 gave useful results for the 1986 Hollister earthquake. Station 3 is a considerable distance away compared to stations 1, 5, and 6 and is not considered in this report. It will be examined later when a suitable multi degree of freedom spectra is completed. Figure 3 shows typical traces of the three components of acceleration measured at station 1 in the directions of 255°, vertical, 345°.

Differential Displacements

The base line correction option which puts a line through the data by minimizing the sum of the squares of the deviations gave unsatisfactory results. As that processing was designed for digitized film records, it was decided that for directly digitized records some modifications were in order. In particular it was noticed that the pre-event memory shows a relatively noise-free portion at the beginning. It was considered that the base line correction needed was the initial zero offset. This was determined by least-square fitting a zero line through the first 1.0 sec of each record and to use this as the base-line correction.

Several filter widths were experimented with in the double integrations of accelerations to give differences of displacements. A filter width or long-period limit of 5 sec. was deemed satisfactory. The displacements at stations at 5 and 6 were rotated to give the components longitudinal and transverse to the leg of the array at 288°. Figures 4, 5, and 6 show the differences of transverse displacements between stations 5-1, 6-1, and 6-5. Figures 7, 8, 9 show the differences of longitudinal displacements between stations 5-1, 6-1, and 6-5. The earthquake was small and the differences in displacement similarly so. Overlays of the displacements shown in figures 10, 11, and 12 for the three components show the similarity of the displacements. The closest stations 5 and 6 show almost equal values.

Differential Spectra

These simple differential spectra have most relevance to shorter structures where the fundamental mode dominates. Stations 5 and 6 are the closest together and have been examined in the most detail. Figures 13, 14, and 15 show the transverse spectra for the special simplified cases $\omega_1 = \omega_2$ and three values of damping, $\lambda = 0$, 0.1, and 0.2. At the smallest values of ω_1, the ratio approaches unity as it should. However as ω_1 increases, representing stiffer structures the ratio R fluctuates and reaches values greater than unity, showing that the differential strains have a considerable effect on the strains developed in the structure. In fact, for damped stiff structures, they dominate over the inertial strains. Figures 16 through 24 show R for various values of ω_2 and λ. Figures 25, 26, and 27 show the spectra for station 5 minus 1 and show the ratio R is substantially larger for greater distances between the stations. Figures 28, 29, 30, 31 show some longitudinal spectra for stations 6 minus 5.

1981 Westmorland Records

Stations 1, 2, 3 of the El Centro Array produced useful records for the 1981 Westmorland earthquake. It was not possible to make the same baseline correction as was done for the Hollister records because the pre-event memory part of the record was not clean enough. The original base line correction was used together with a uni-directional high pass Butterworth filter with a six second cut off. The resulting phase change was deemed acceptable.

Differential Displacements

Figures 32, 33, and 34 show the differences of displacements between stations 1, 2 and 3 in the transverse directions. Figures 35, 36, and 37 show the difference of displacements in the longitudinal direction. Figures 38, 39, and 40, show the transverse spectra, channel 2, for the two closest stations 1 and 2 for different values of damping; the magnification is relatively small. Figures 41, 42, and 43 show the spectra for values $\omega_2 = 20$ and different damping values. Again, the magnification is relatively small. Spectra for the differences between the other stations show no particular change in character and are not reported.

Conclusions

Differential strains impressed on a structure will, in certain circumstances, add significant strains to the inertial strains developed in a structure subjected to an earthquake. The development of multi-degree-of-freedom differential spectra will show more effectively the significance of differential loadings on structures.

References

Bycroft, G.N., 1980, Soil foundation interaction and differential ground motions: Journal of Earthquake Engineering and Structural Dynamics, v. 8, no. 5, p. 397-404.

Bycroft, G.N., 1982, El Centro differential ground motion array: U.S. Geological Survey Professional Paper 1254, p. 351-356.

Bycroft, G.N., 1983, Differential ground motion array at Hollister Municipal Airport, California: U.S. Geological Survey Open-File Report No. 83-327.

Converse, A.M., 1984, AGRAM: A series of computer programs for processing digitized strong-motion accelerograms, version 2.0: U.S. Geological Survey Open File Report 84-525, 118 p.

Trifunac, M.D., 1972, Interaction of a shear wall with the soil for incident plane SH waves: Seismological Society of America Bulletin, v. 62, no. 1, p. 63-83.

Wong, H.L., and Trifunac, M.D., 1974, Interaction of a shear wall with the soil for incident plane SH waves: Elliptical rigid foundation: Seismological Society of America Bulletin, v. 64, no. 6., p. 1825-1842.

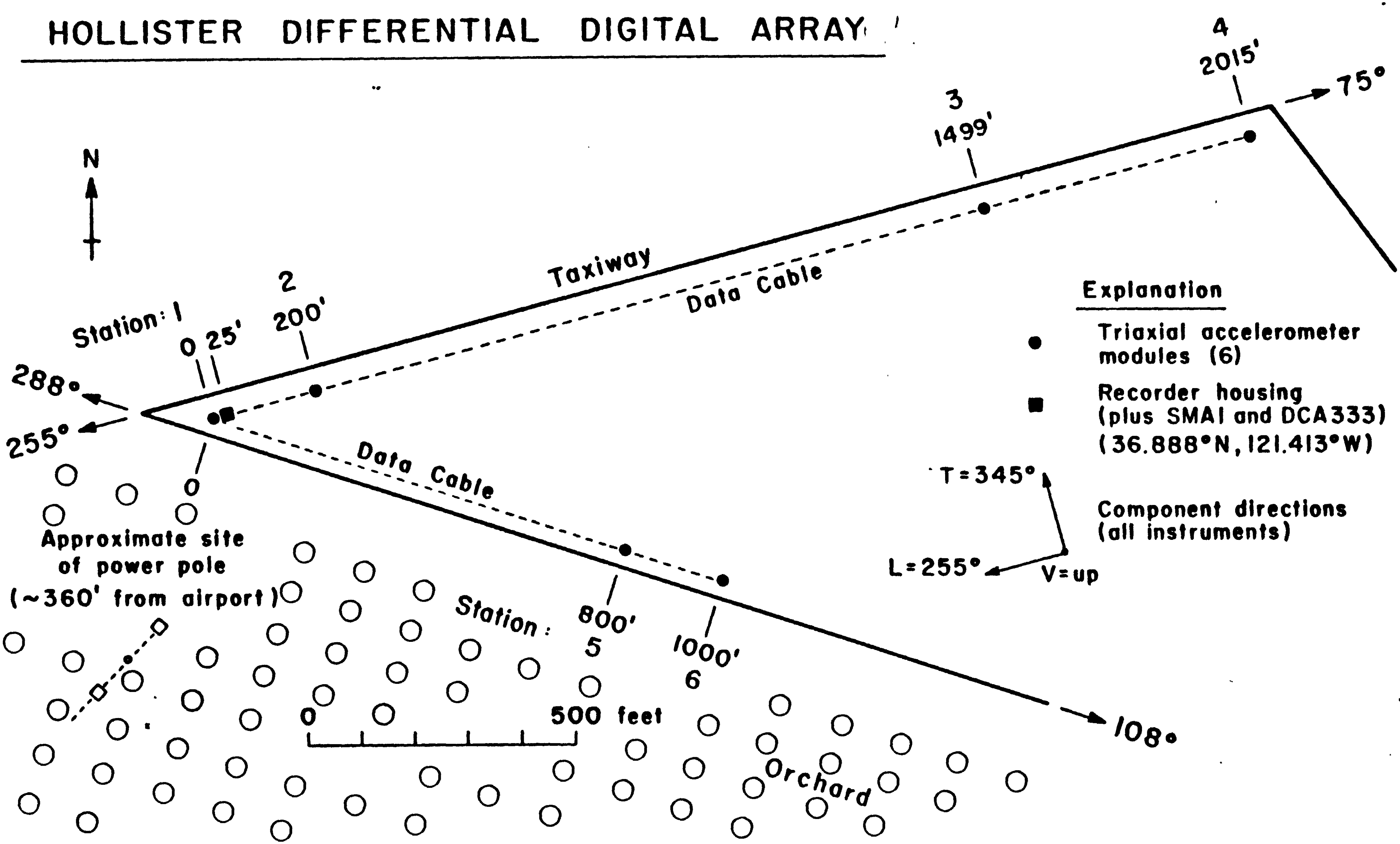
HOLLISTER DIFFERENTIAL DIGITAL ARRAY
N
Station: 1
0 25'
2
200'
3
1499'
4
2015'
75°
288°
255°
108°
0
Taxiway
Data Cable
Data Cable
Station:
800'
5
1000'
6
Approximate site
of power pole
(~360' from airport)
0
500 feet
Orchard
Explanation
Triaxial accelerometer
modules (6)
Recorder housing
(plus SMA1 and DCA333)
(36.888°N, 121.413°W)
T=345°
L=255°
V=up
Component directions
(all instruments)

FIGURE 1

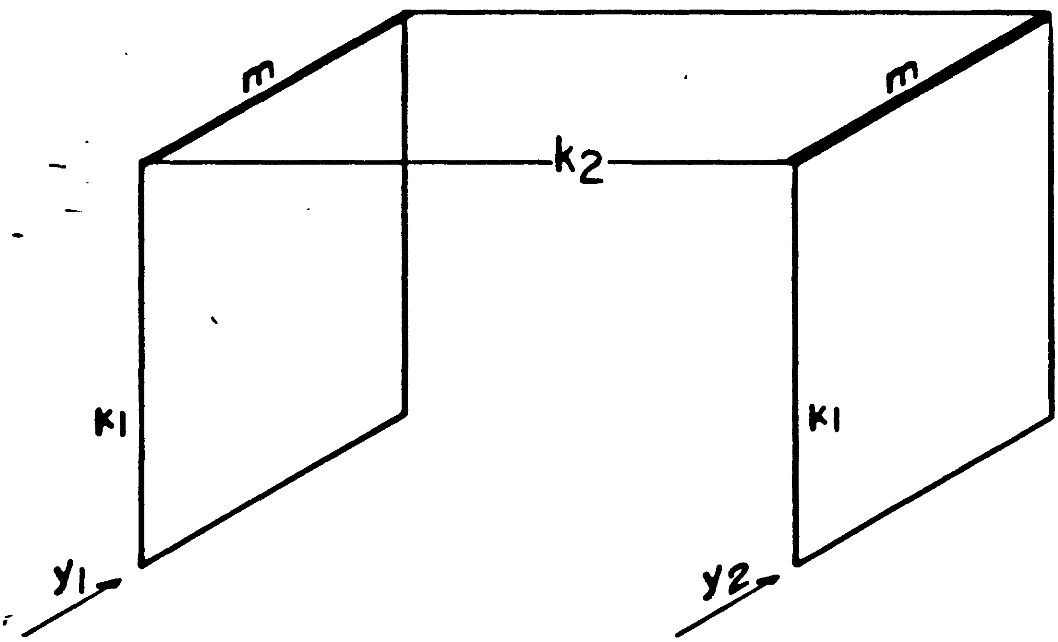

Figure 2. Model for differential spectra.

UNCORRECTED ACCELEROGRAM
HOLLISTER, DIFFERENTIAL ARRAY NO 1
255 DEGREES, UP, 345 DEGREES
EARTHQUAKE OF JANUARY 26, 1986, 1920:50.9 GMT
PEAK VALUES (CM/SEC/SEC): 92.80 168.21 104.06

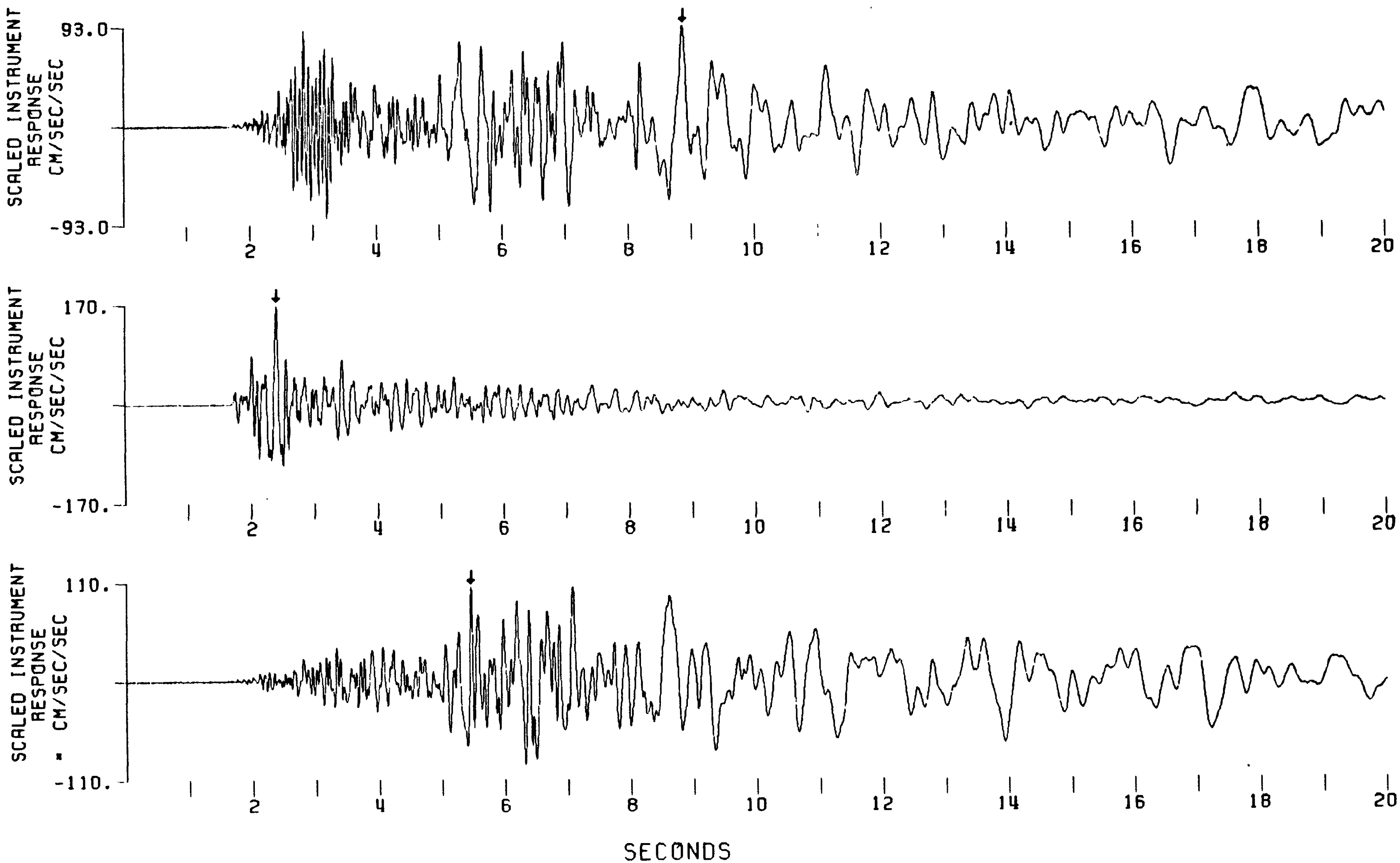

Fig 3

HOLLISTER, DIFFERENTIAL ARRAY: TRANSVERSE (18 DEGREE) COMPONENT
NO 5 MINUS NO 1, NO 6 MINUS NO 1, NO 6 MINUS NO 5
EARTHQUAKE OF JANUARY 26, 1986, 1920:50.9 GMT
BASELINE COR. FROM 0.0 TO 1.0 SEC, BUTTERWORTH FILTER AT .200 HZ, ORDER 2

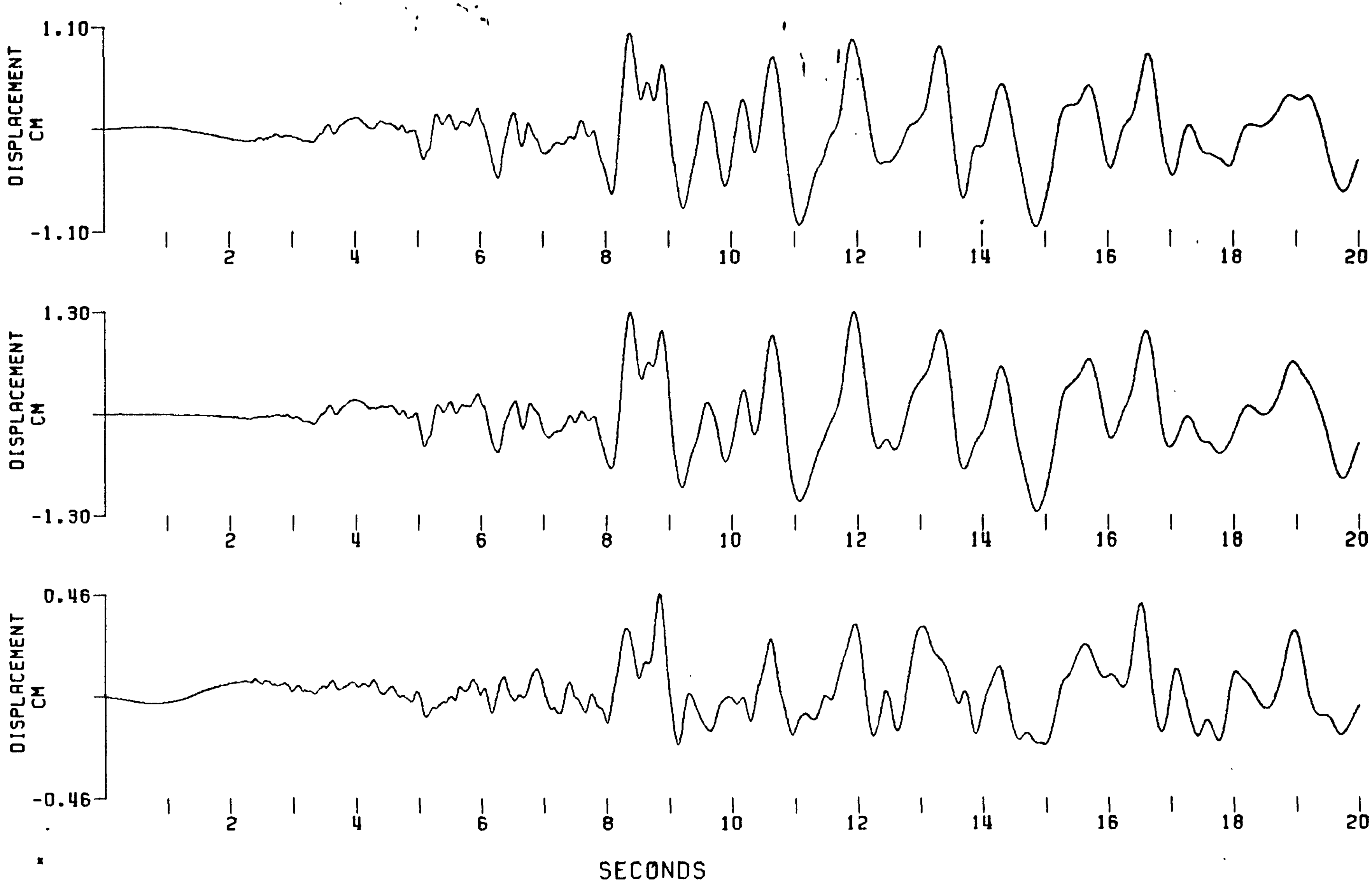

Fig 4

HOLLISTER, DIFFERENTIAL ARRAY: TRANSVERSE (18 DEGREE) COMPONENT
NO 5 MINUS NO 1, NO 6 MINUS NO 1, NO 6 MINUS NO 5
EARTHQUAKE OF JANUARY 26, 1986, 1920:50.9 GMT
BASELINE COR. FROM 0.0 TO 1.0 SEC, BUTTERWORTH FILTER AT .200 HZ, ORDER 2

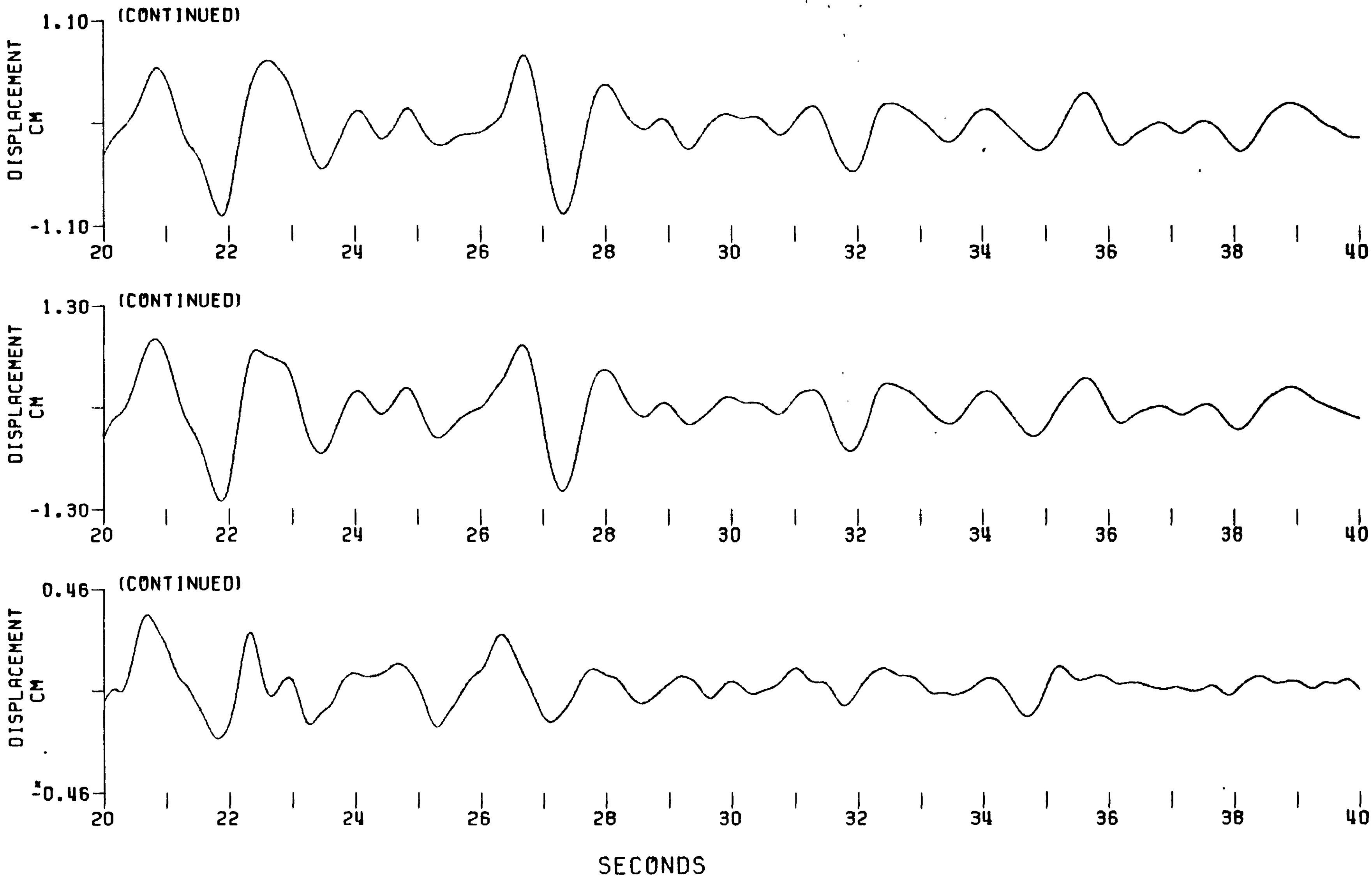

Fig 5

HOLLISTER, DIFFERENTIAL ARRAY: TRANSVERSE (18 DEGREE) COMPONENT
NO 5 MINUS NO 1, NO 6 MINUS NO 1, NO 6 MINUS NO 5
EARTHQUAKE OF JANUARY 26, 1986, 1920:50.9 GMT
BASELINE COR. FROM 0.0 TO 1.0 SEC, BUTTERWORTH FILTER AT .200 HZ, ORDER 2

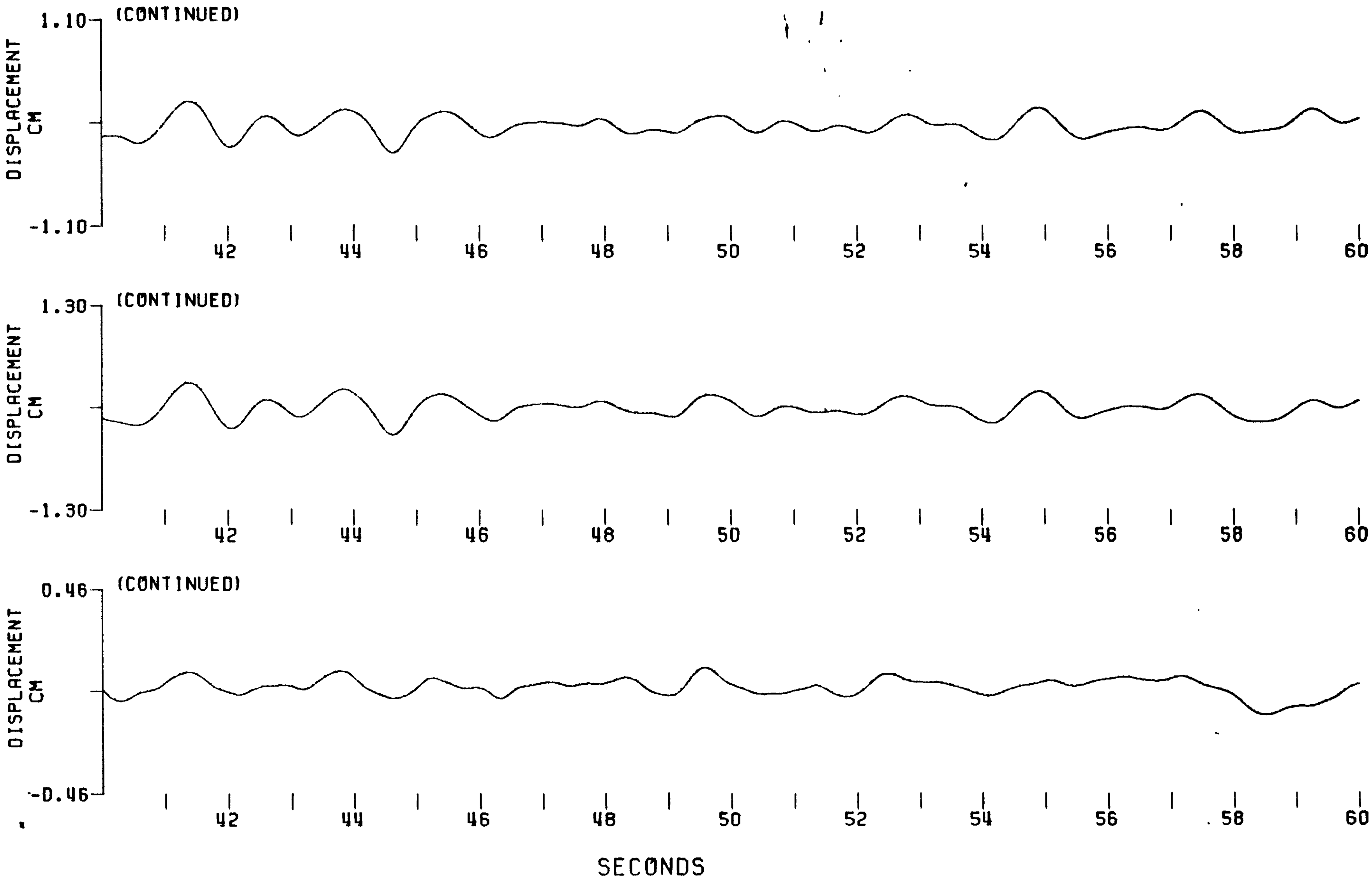

Fig 6

HOLLISTER, DIFFERENTIAL ARRAY: LONGITUDINAL (288 DEGREE) COMPONENT
NO 5 MINUS NO 1, NO 6 MINUS NO 1, NO 6 MINUS NO 5
EARTHQUAKE OF JANUARY 26, 1986, 1920:50.9 GMT
BASELINE COR. FROM 0.0 TO 1.0 SEC, BUTTERWORTH FILTER AT .200 HZ, ORDER 2

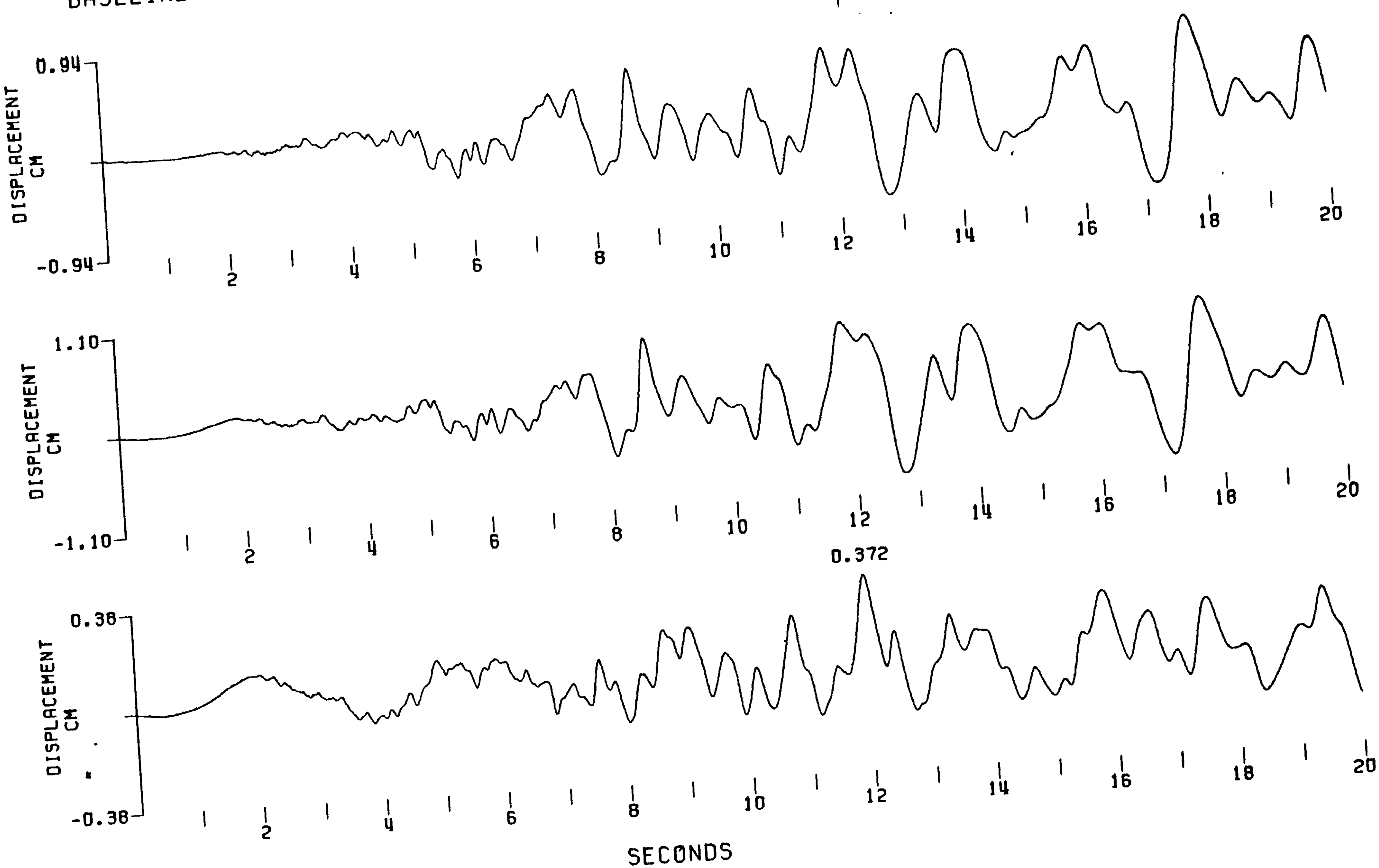

Fig 7

HOLLISTER, DIFFERENTIAL ARRAY: LONGITUDINAL (288 DEGREE) COMPONENT
NO 5 MINUS NO 1, NO 6 MINUS NO 1, NO 6 MINUS NO 5
EARTHQUAKE OF JANUARY 26, 1986, 1920:50.9 GMT
BASELINE COR. FROM 0.0 TO 1.0 SEC, BUTTERWORTH FILTER AT .200 HZ, ORDER 2

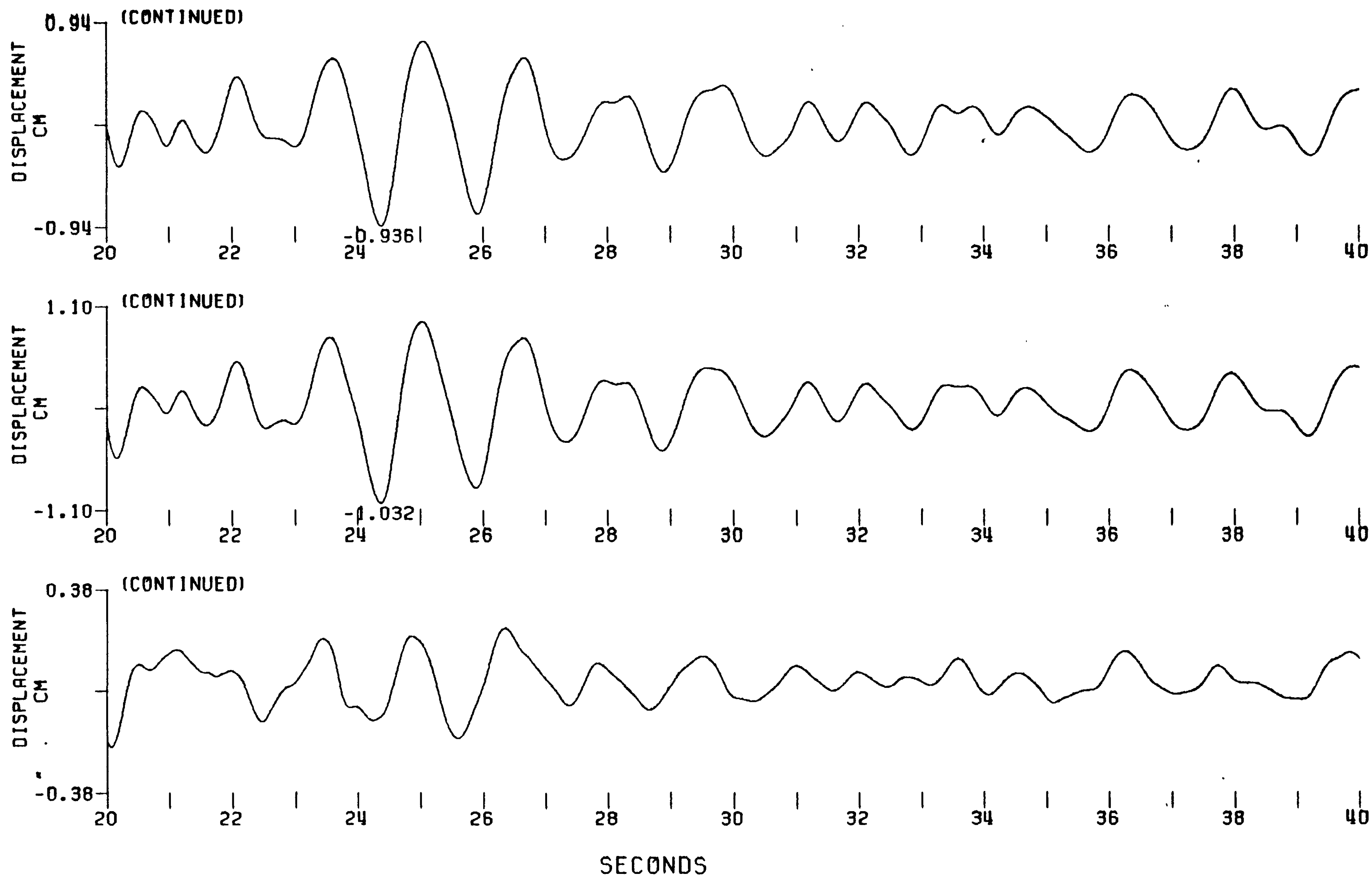

Fig 8

HOLLISTER, DIFFERENTIAL ARRAY: LONGITUDINAL (288 DEGREE) COMPONENT
NO 5 MINUS NO 1, NO 6 MINUS NO 1, NO 6 MINUS NO 5
EARTHQUAKE OF JANUARY 26, 1986, 1920:50.9 GMT
BASELINE COR. FROM 0.0 TO 1.0 SEC, BUTTERWORTH FILTER AT .200 HZ, ORDER 2

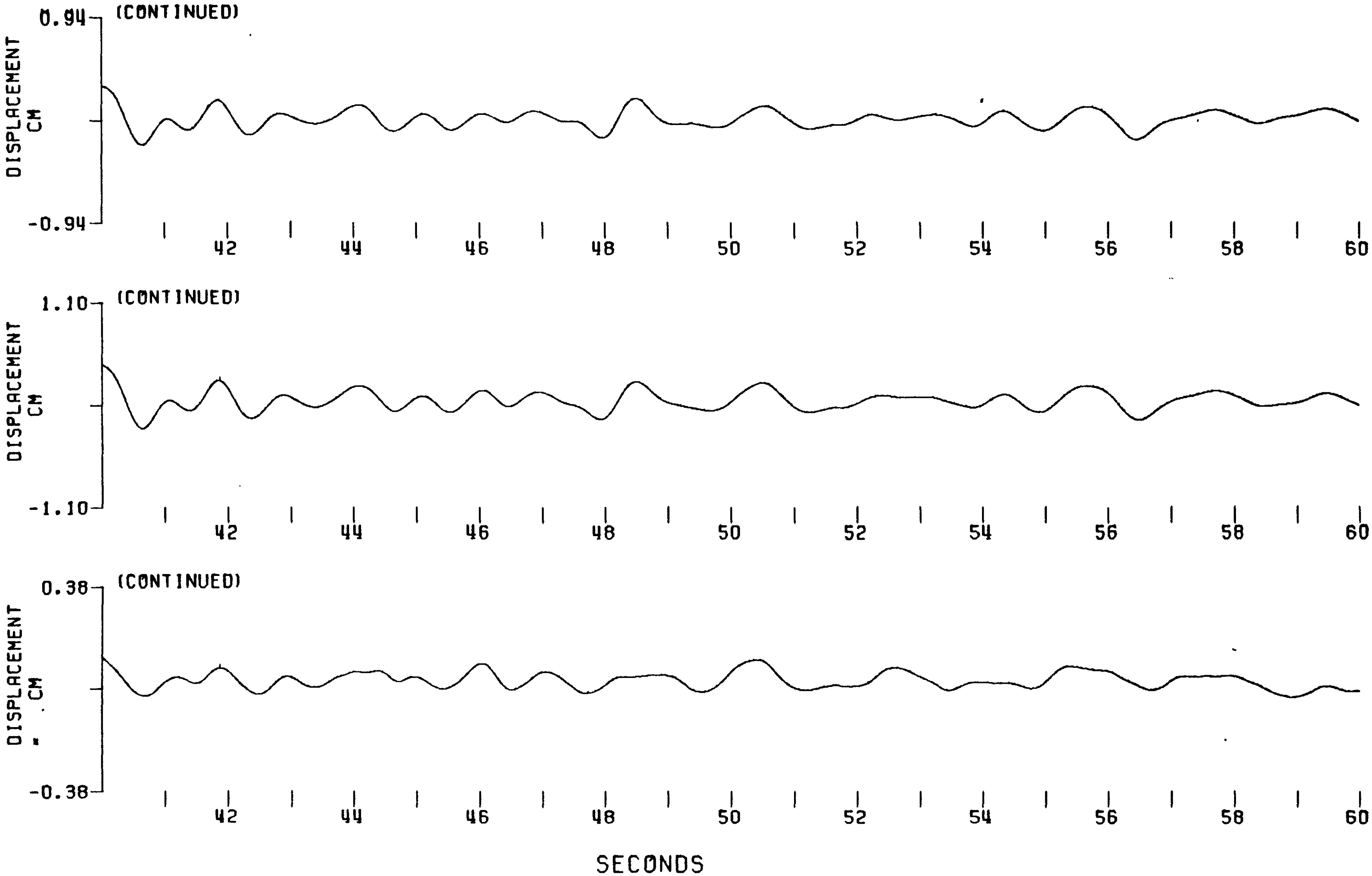

Fig 9

Figure 10. Overlays of displacements for the three components of stations 5 and 6, 1986 Hollister.

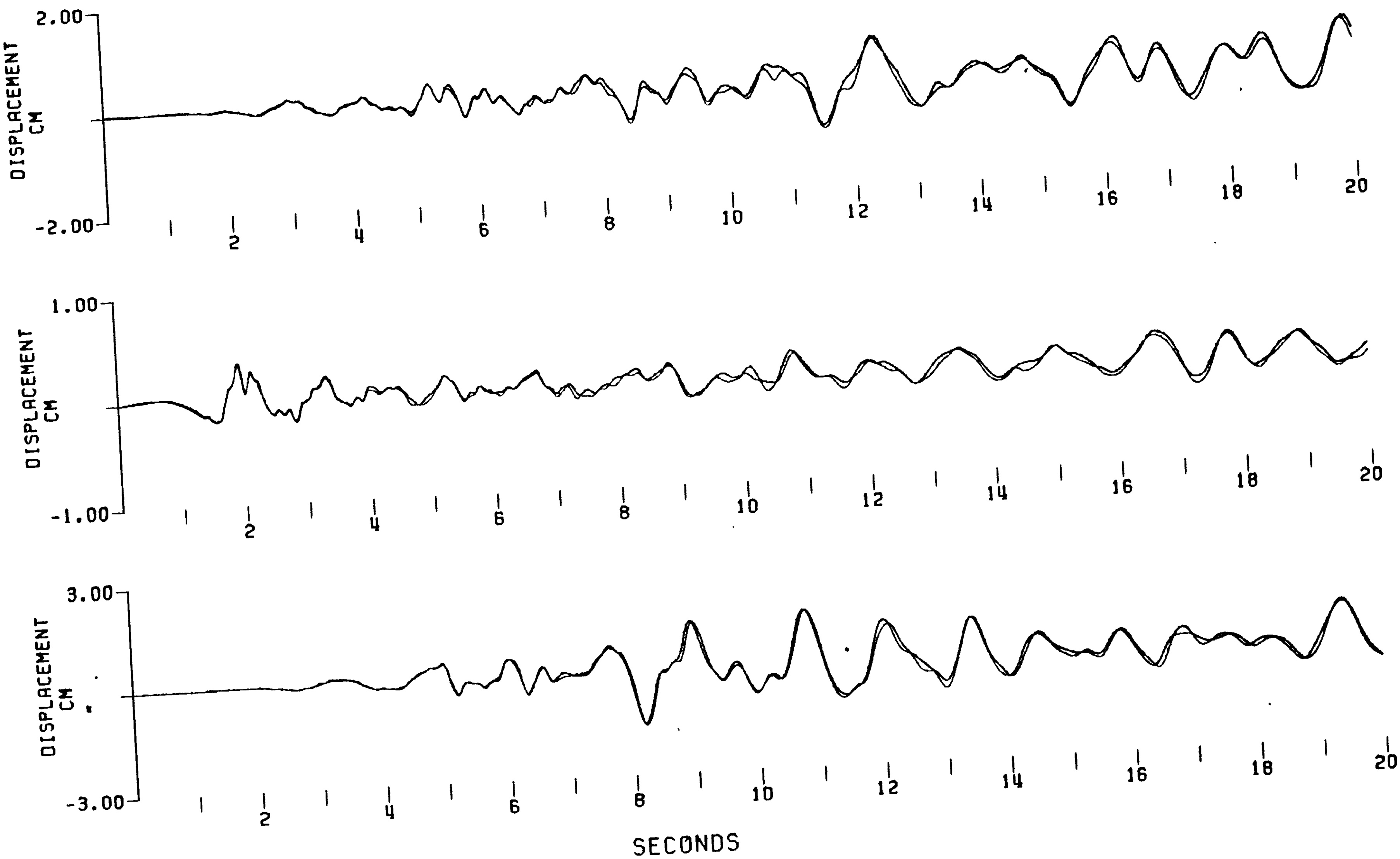

Fig 10

Figure 11. Overlays of displacements for the three components of stations 1 and 6, 1986 Hollister.

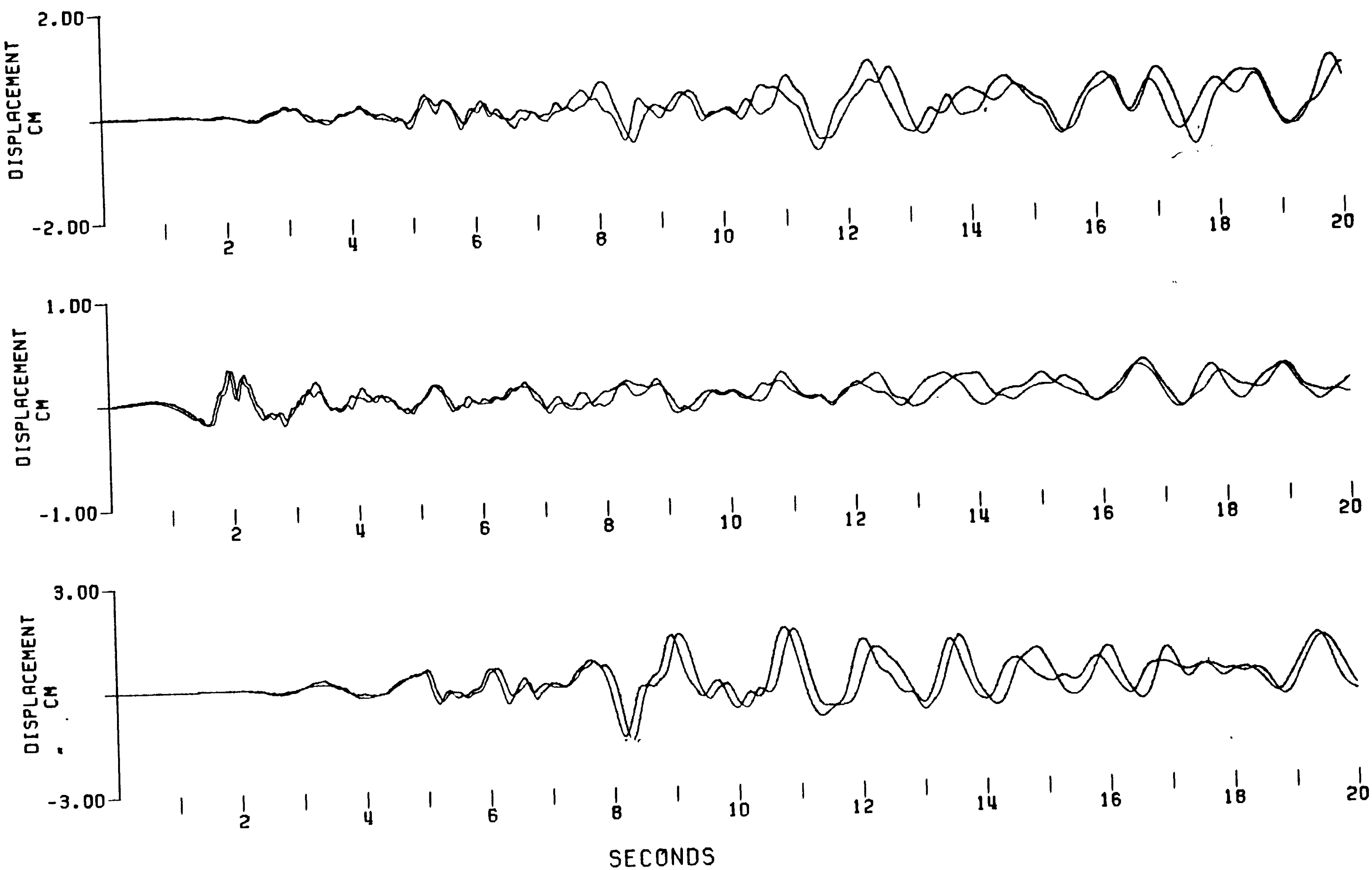

Fig 11

Figure 12. Overlays of displacements for the three components of stations 1 and 5, 1986 Hollister.

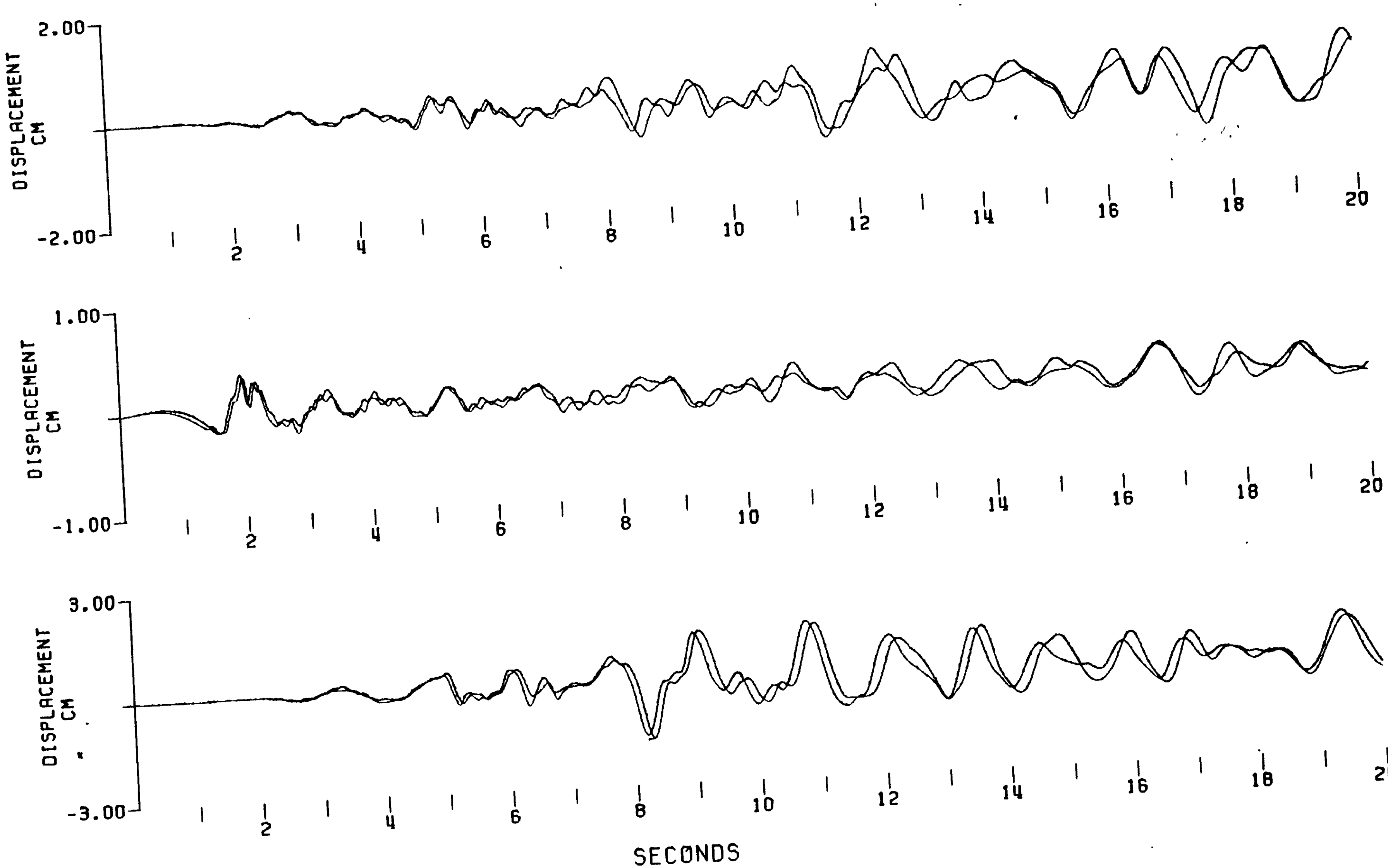

Fig 12

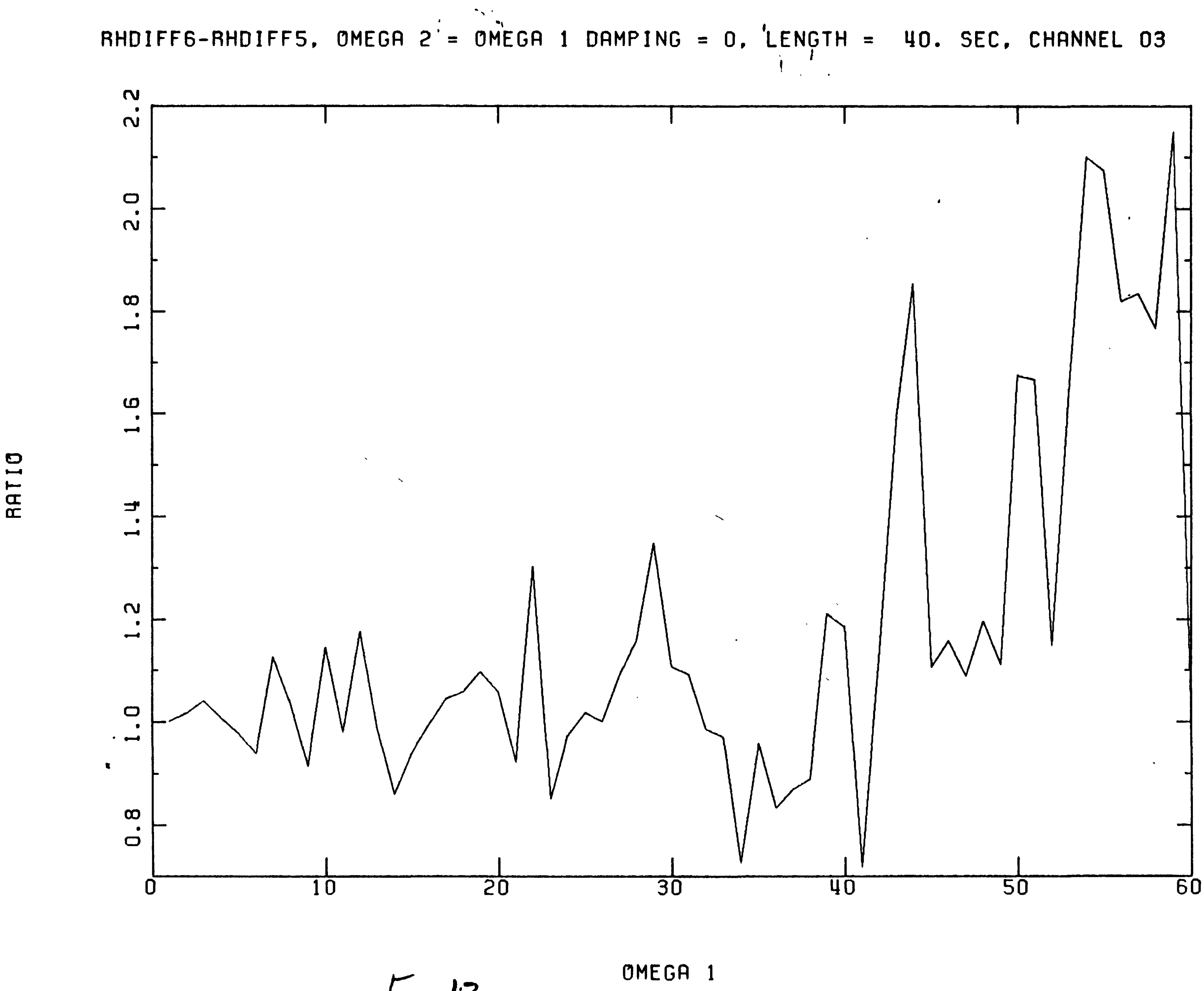
RHDIFF6-RHDIFF5, OMEGA 2 = OMEGA 1 DAMPING = 0, LENGTH = 40. SEC, CHANNEL 03
RATIO
0.8
1.0
1.2
1.4
1.6
1.8
2.0
2.2
0
10
20
30
40
50
60
OMEGA 1

Fig 13

RHDIFF6-RHDIFF5, ØMEGA 2 = ØMEGA 1 DAMPING = 0.1, LENGTH = 40. SEC, CHANNEL 03

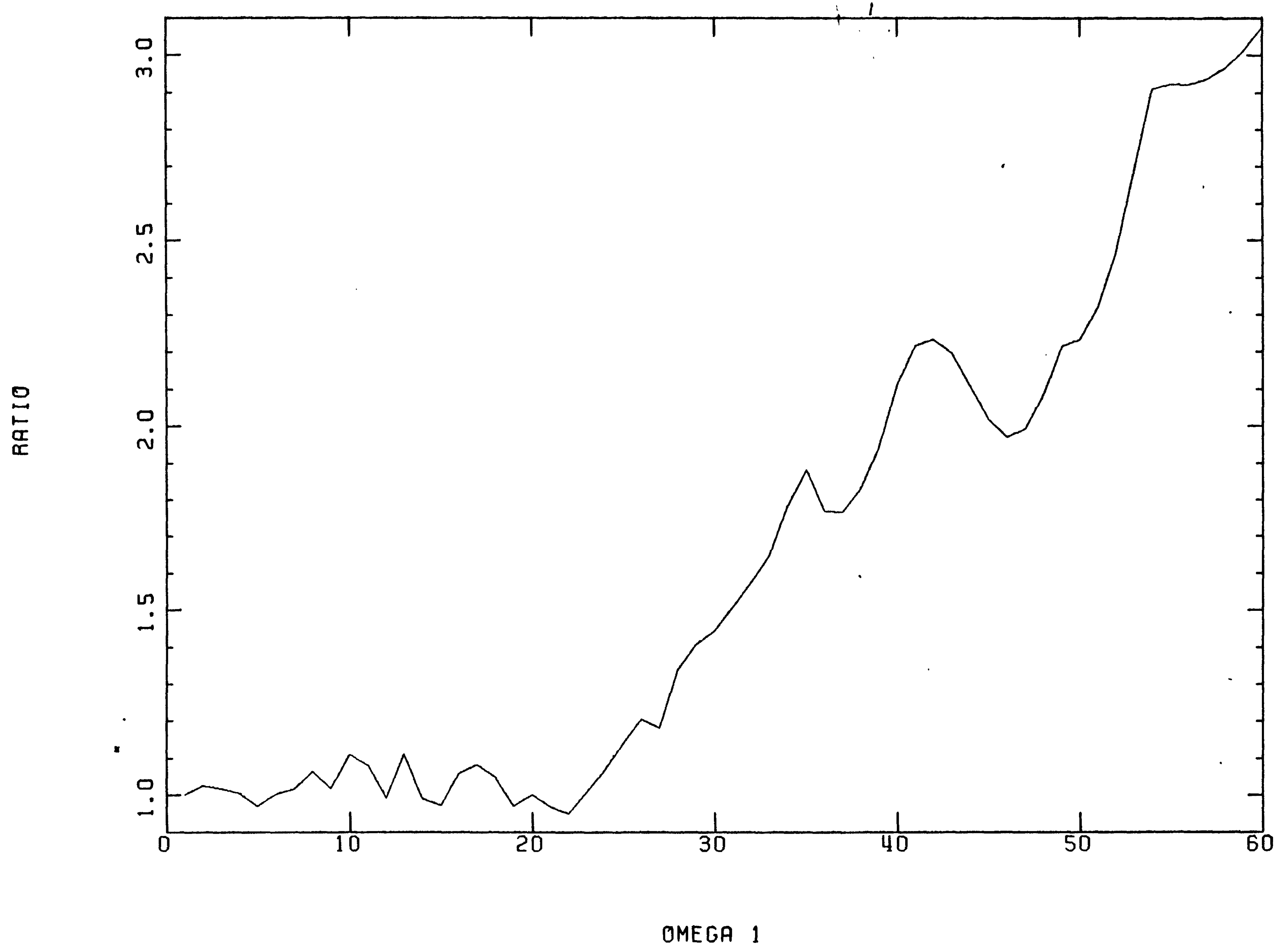

Fig 14

RHDIFF6-RHDIFF5, OMEGA 2 = OMEGA 1 DAMPING = 0.2, LENGTH = 40. SEC, CHANNEL 03

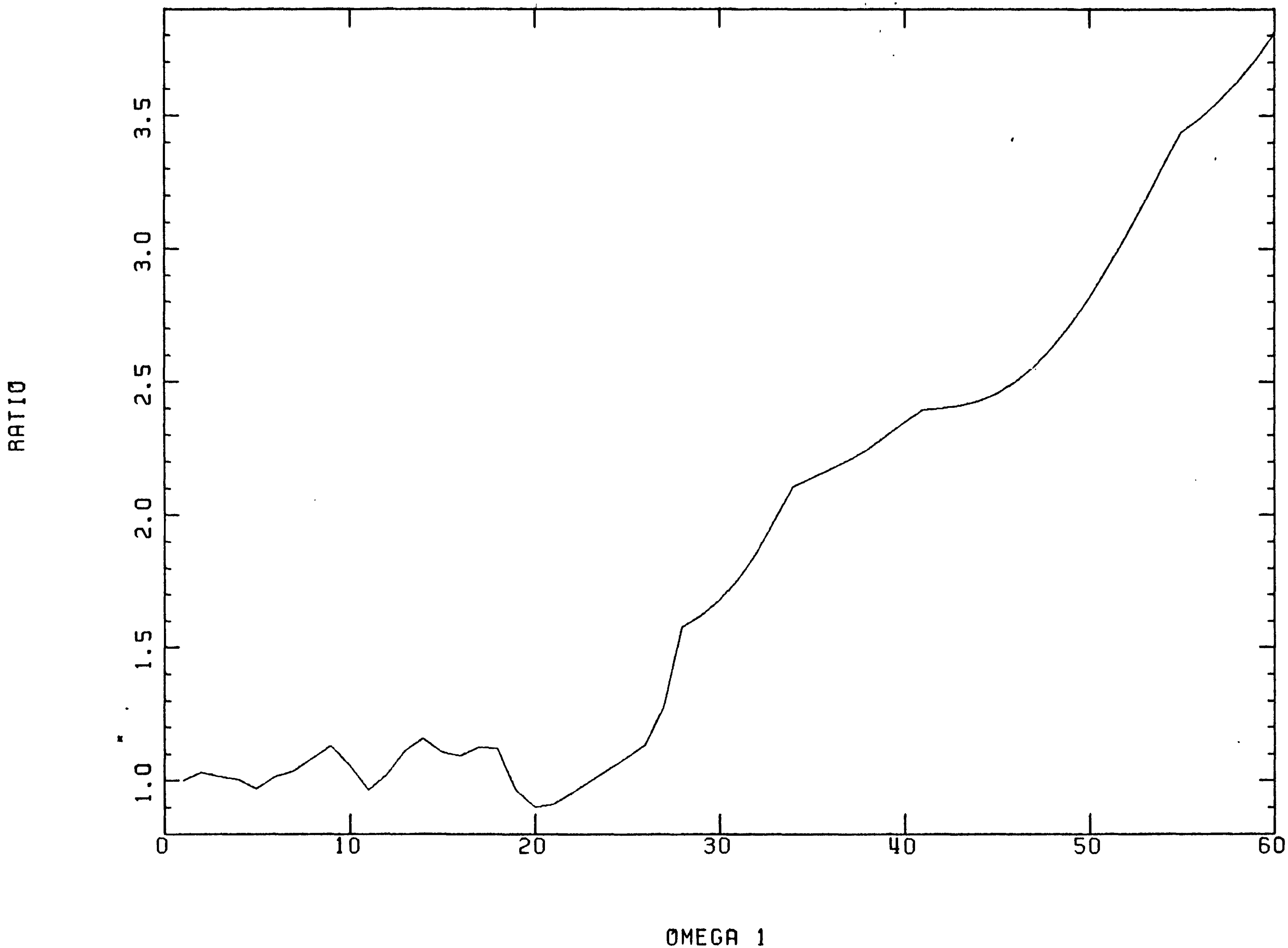

Fig 15

RHDIFF6-RHDIFF5, ØMEGA 2 = 10. DAMPING = 0.0, LENGTH = 40. SEC, CHANNEL 03

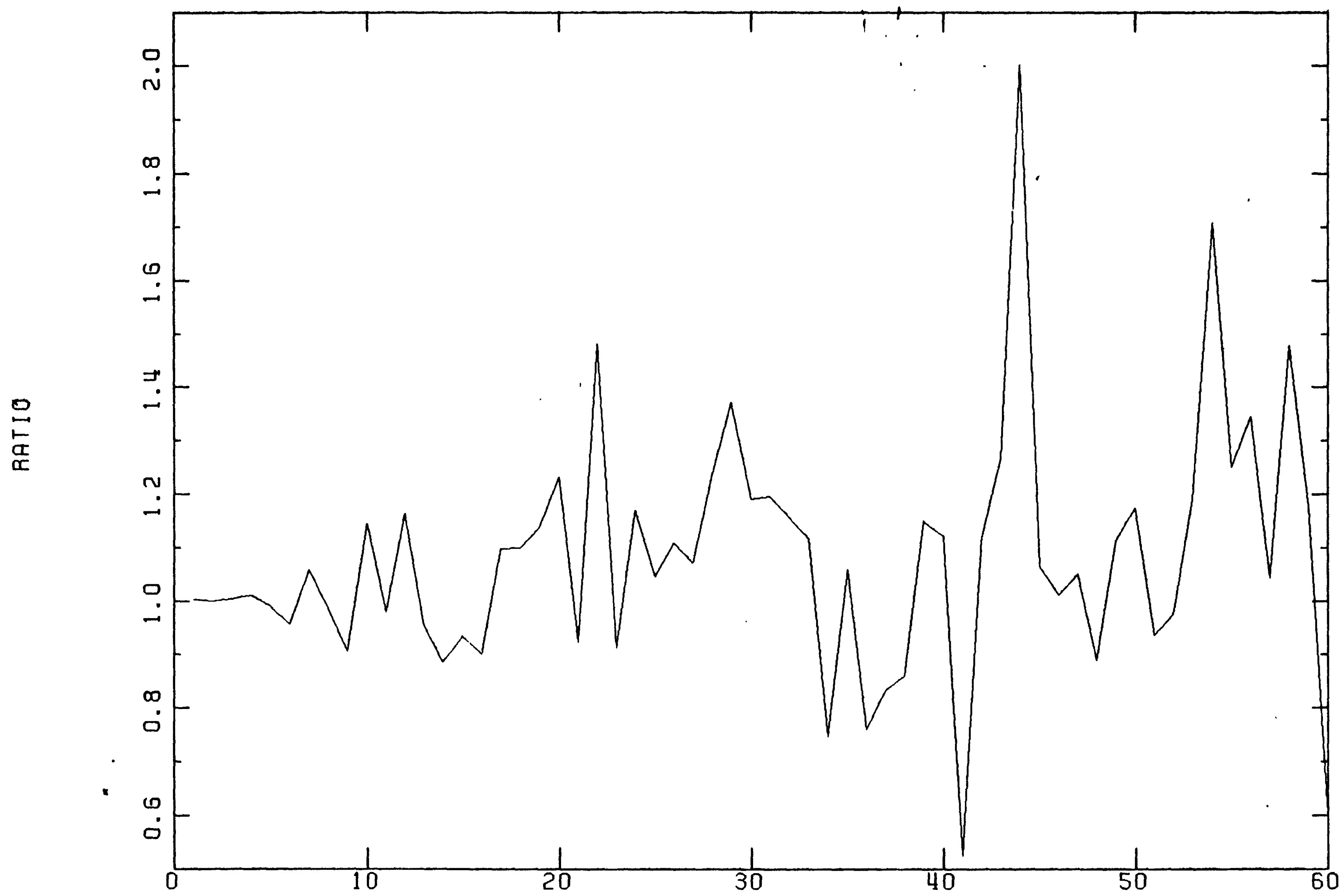

Fig 16

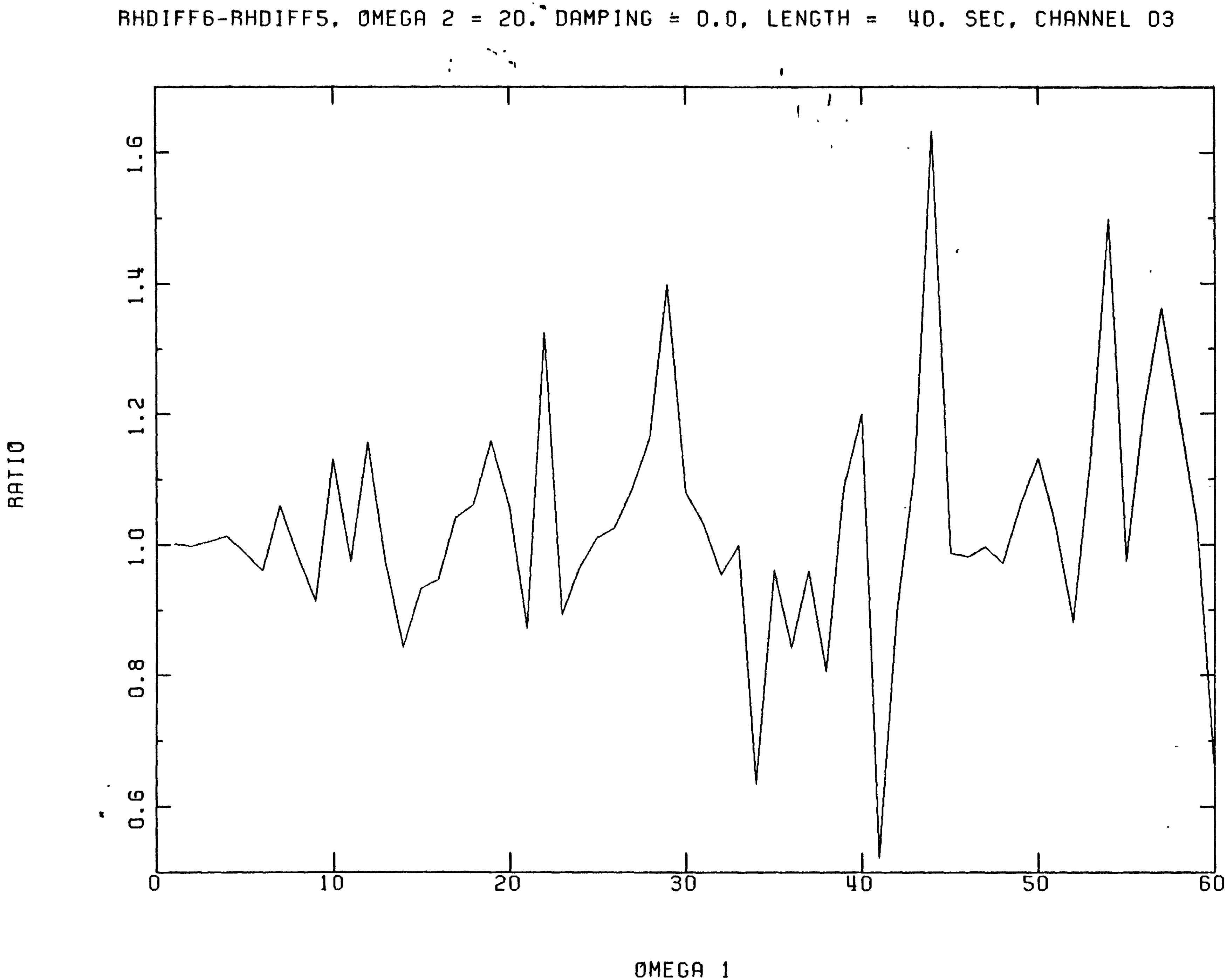
RHDIFF6-RHDIFF5, ØMEGA 2 = 20. DAMPING = 0.0, LENGTH = 40. SEC, CHANNEL 03
RATIO
0.6
0.8
1.0
1.2
1.4
1.6
0
10
20
30
40
50
60
ØMEGA 1

Fig 17

RHDIFF6-RHDIFF5, OMEGA 2 = 30. DAMPING = 0.0, LENGTH = 40. SEC, CHANNEL 03

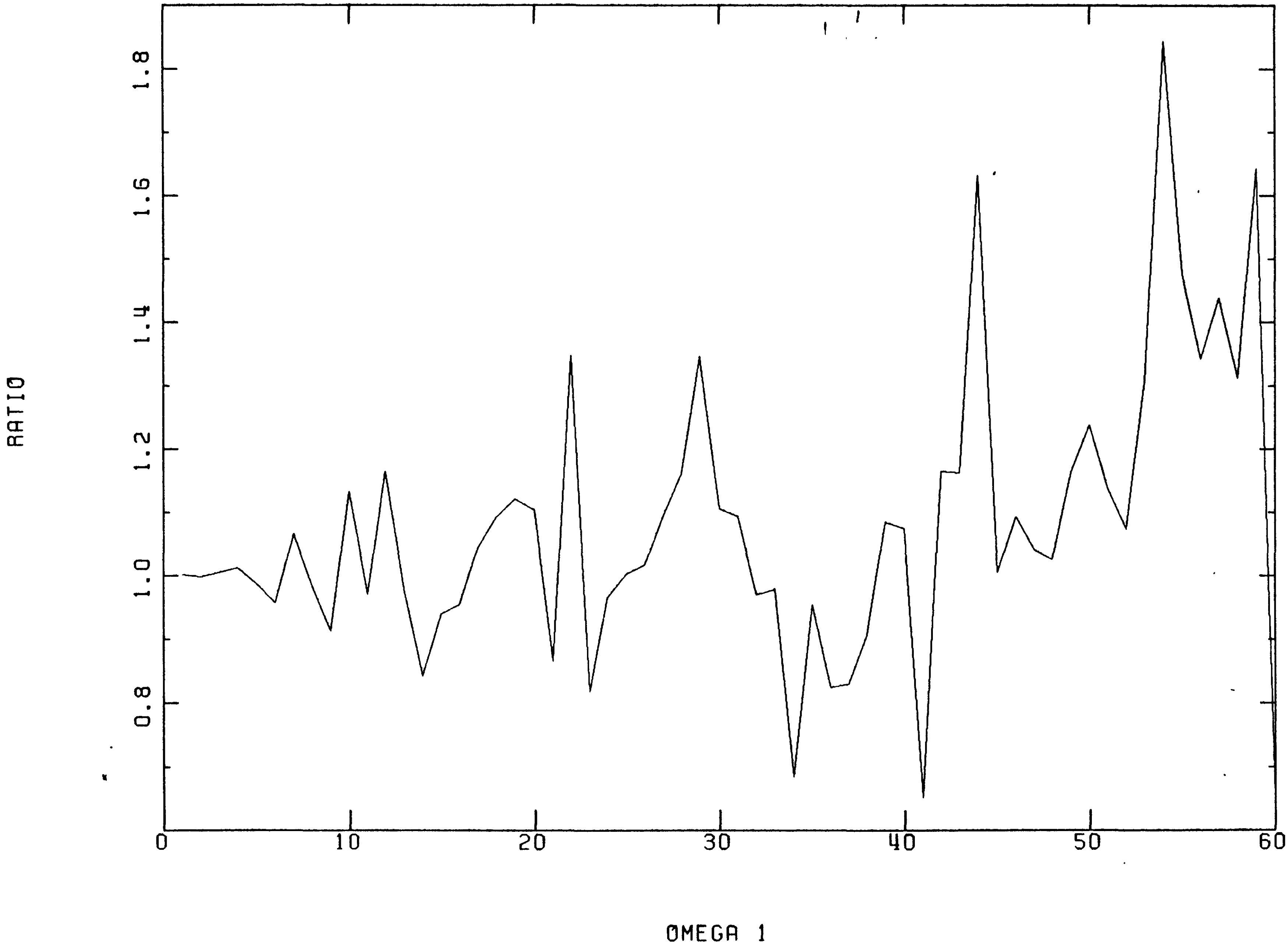

Fig 18

RHDIFF6-RHDIFF5, OMEGA 2 = 10. DAMPING = 0.1, LENGTH = 40. SEC, CHANNEL 03

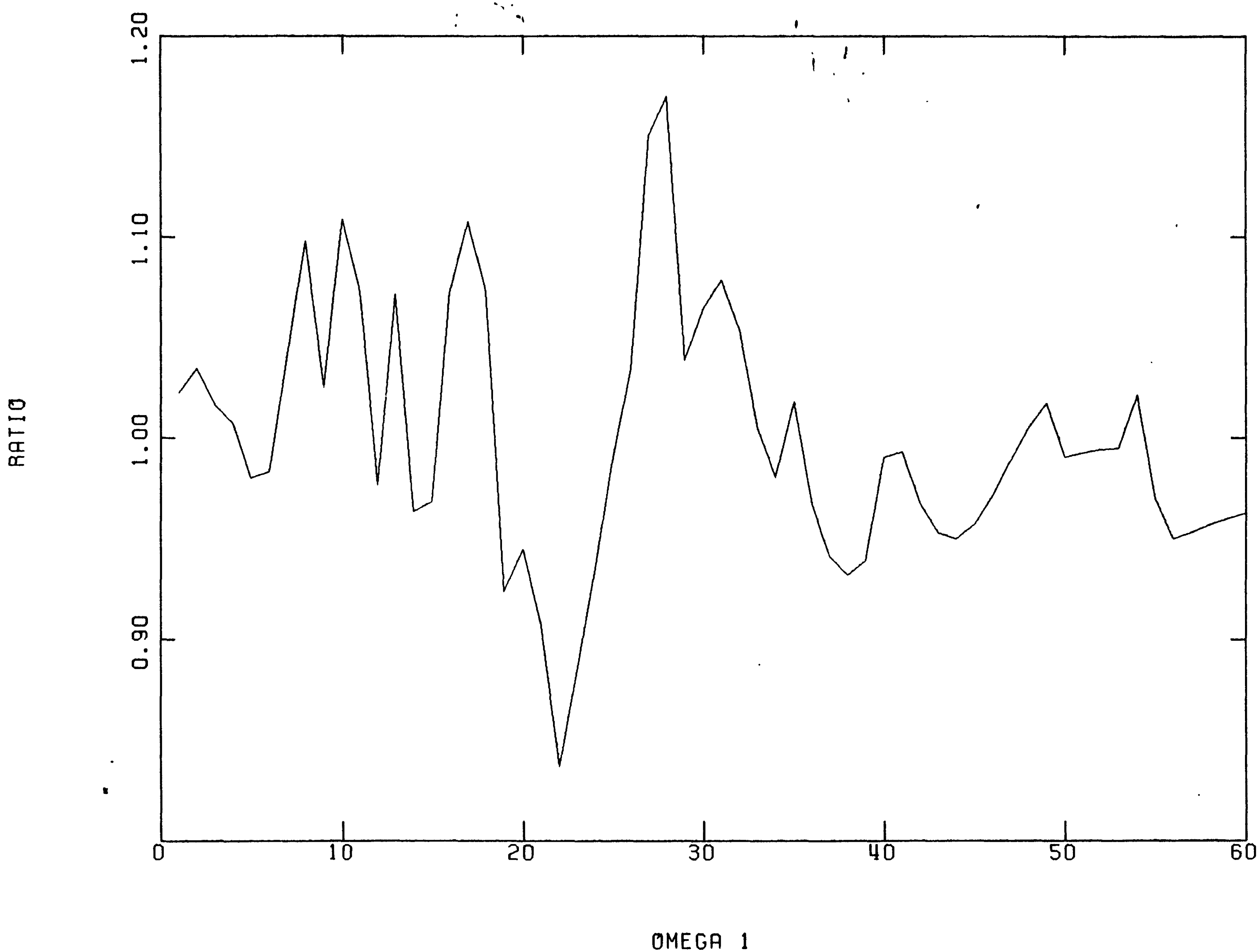

Fig 19

RHDIFF6-RHDIFF5, ØMEGA 2 = 20. DAMPING = 0.1, LENGTH = 40. SEC, CHANNEL 03

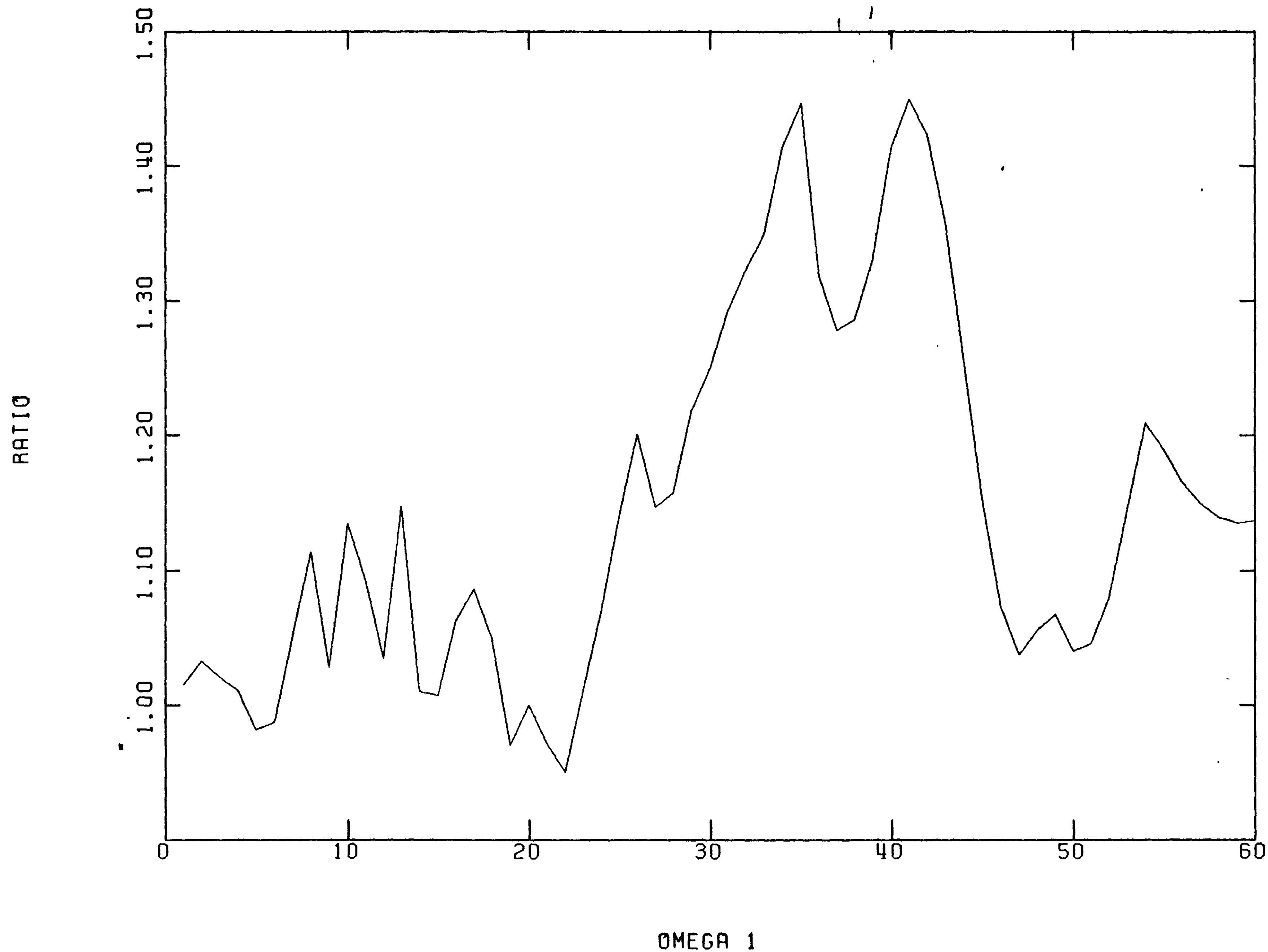

Fig 20

RHDIFF6-RHDIFF5, ØMEGA 2 = 30. DAMPING = 0.1, LENGTH = 40. SEC, CHANNEL 03

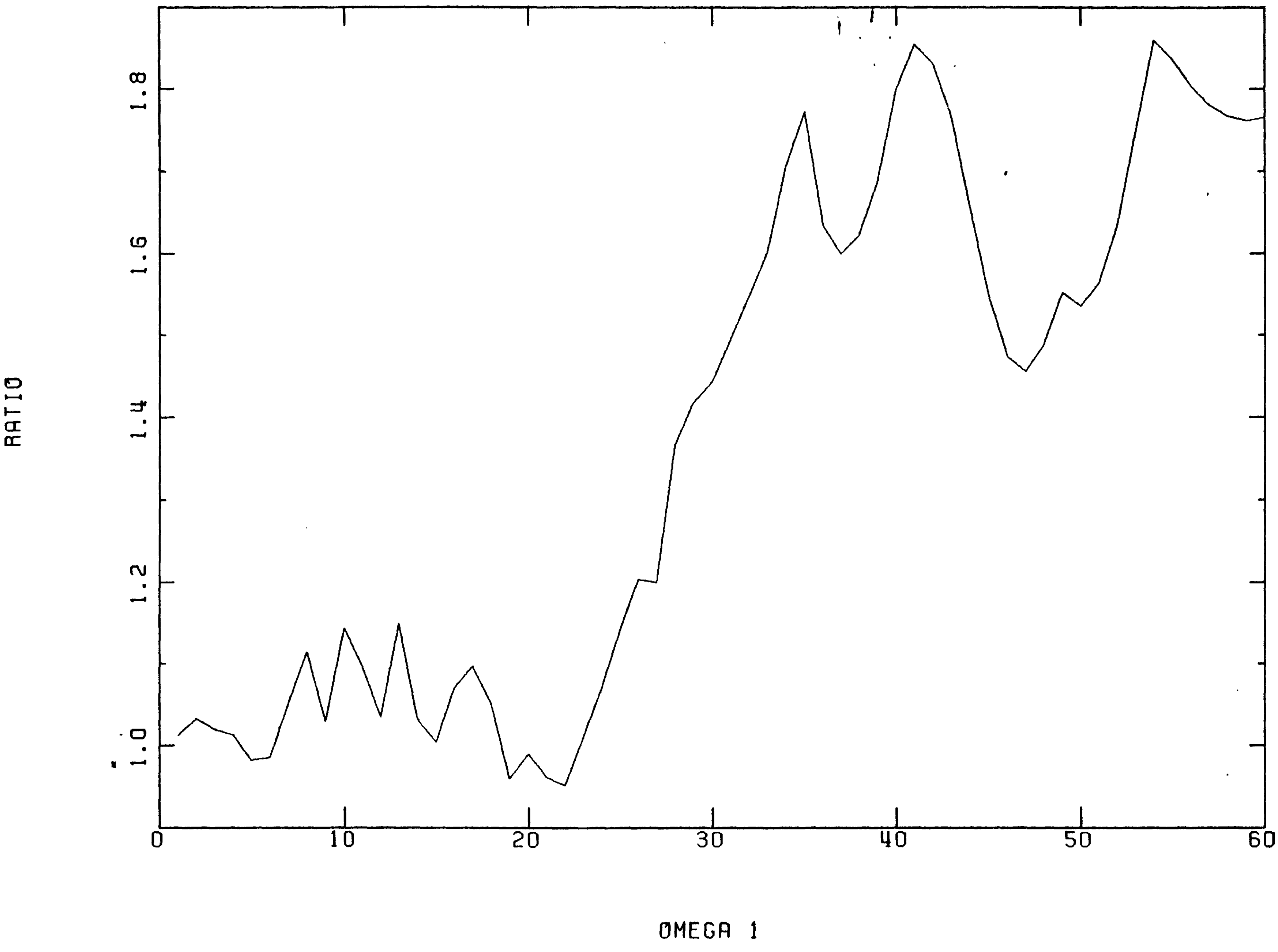

Fig 21

RHDIFF6-RHDIFF5, ØMEGA 2 = 10. DAMPING = 0.2, LENGTH = 40. SEC, CHANNEL 03

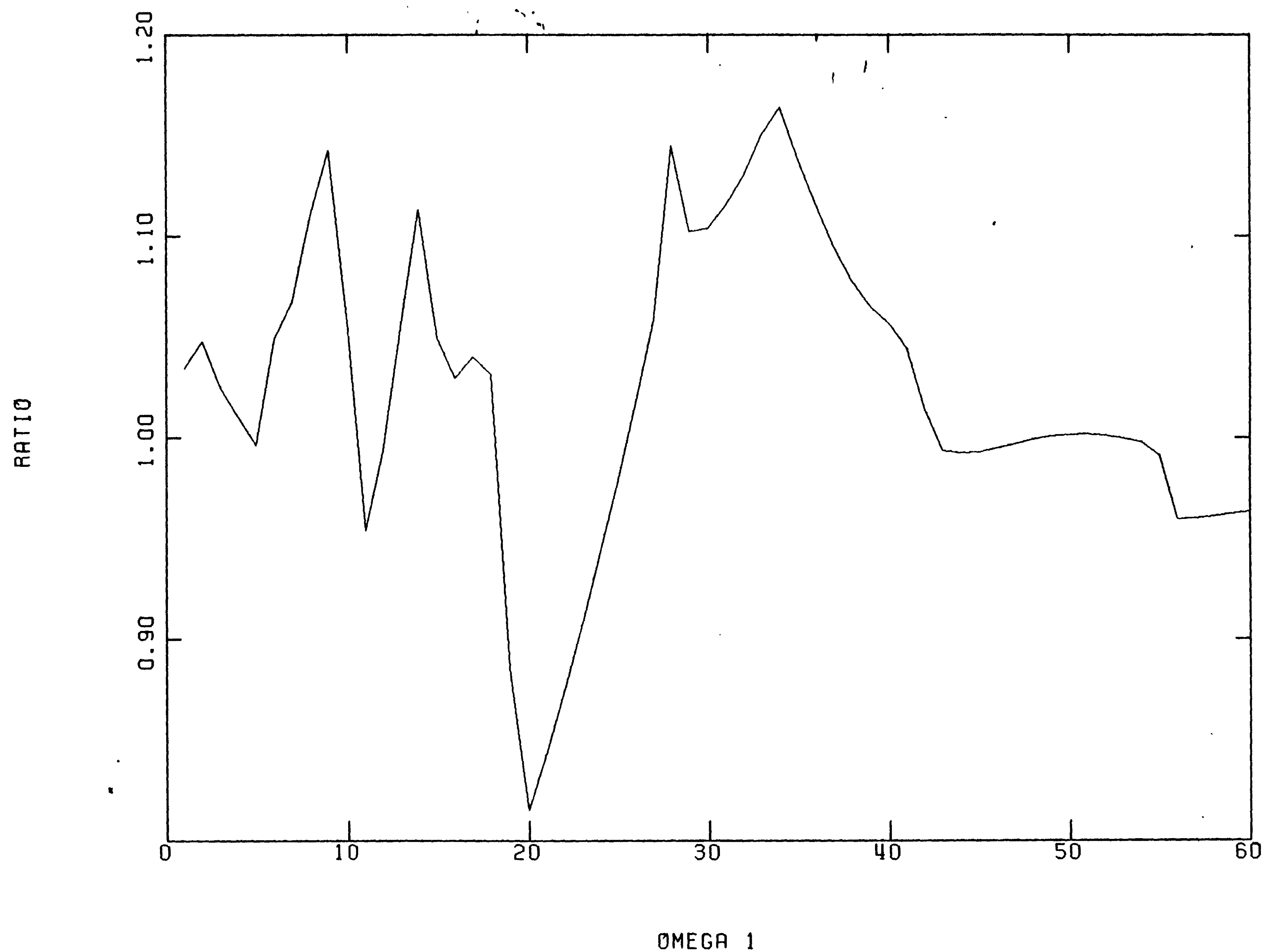

Fig 22

RHDIFF6-RHDIFF5, OMEGA 2 = 20. DAMPING = 0.2, LENGTH = 40. SEC, CHANNEL 03

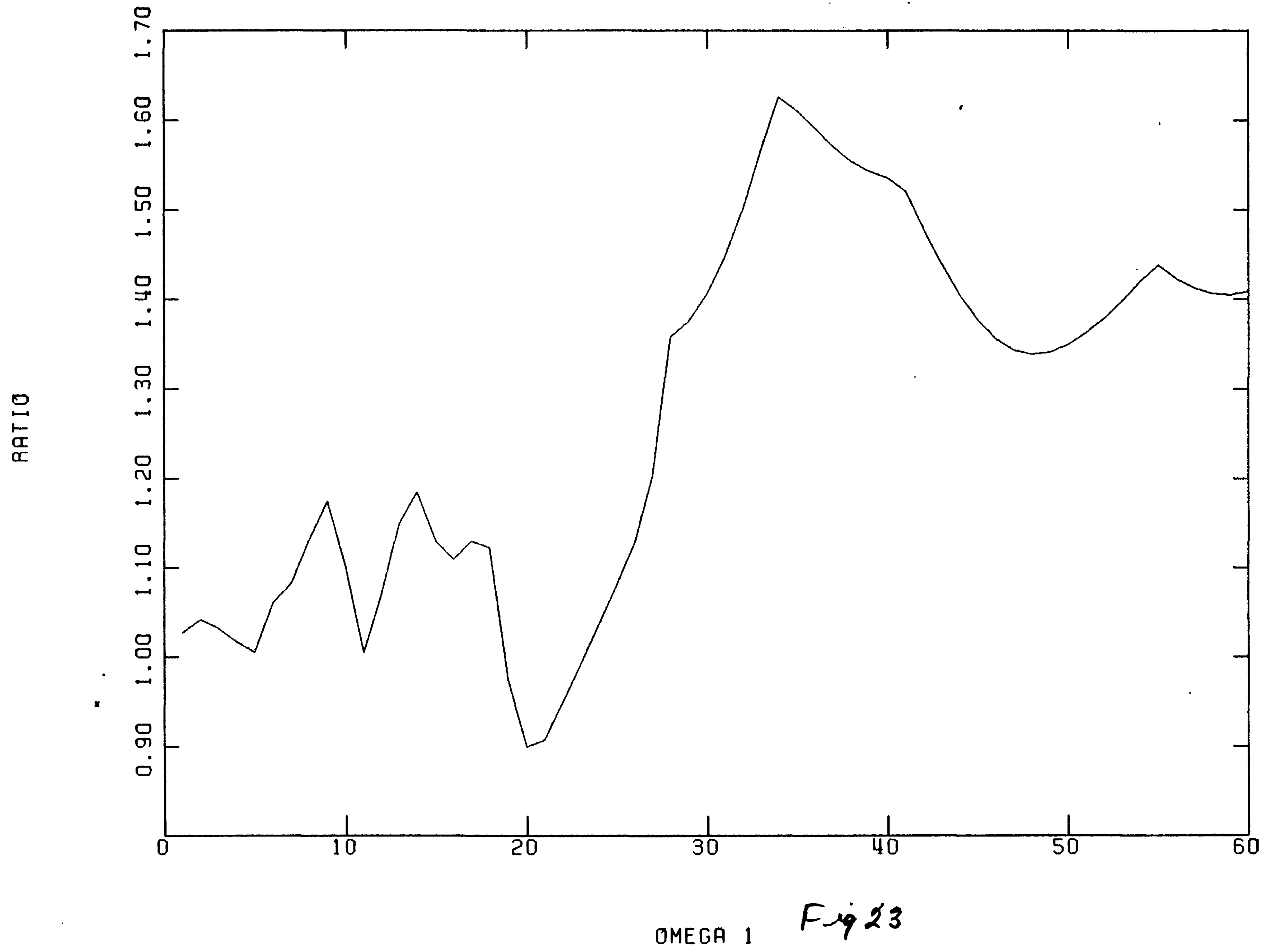

Fig 23

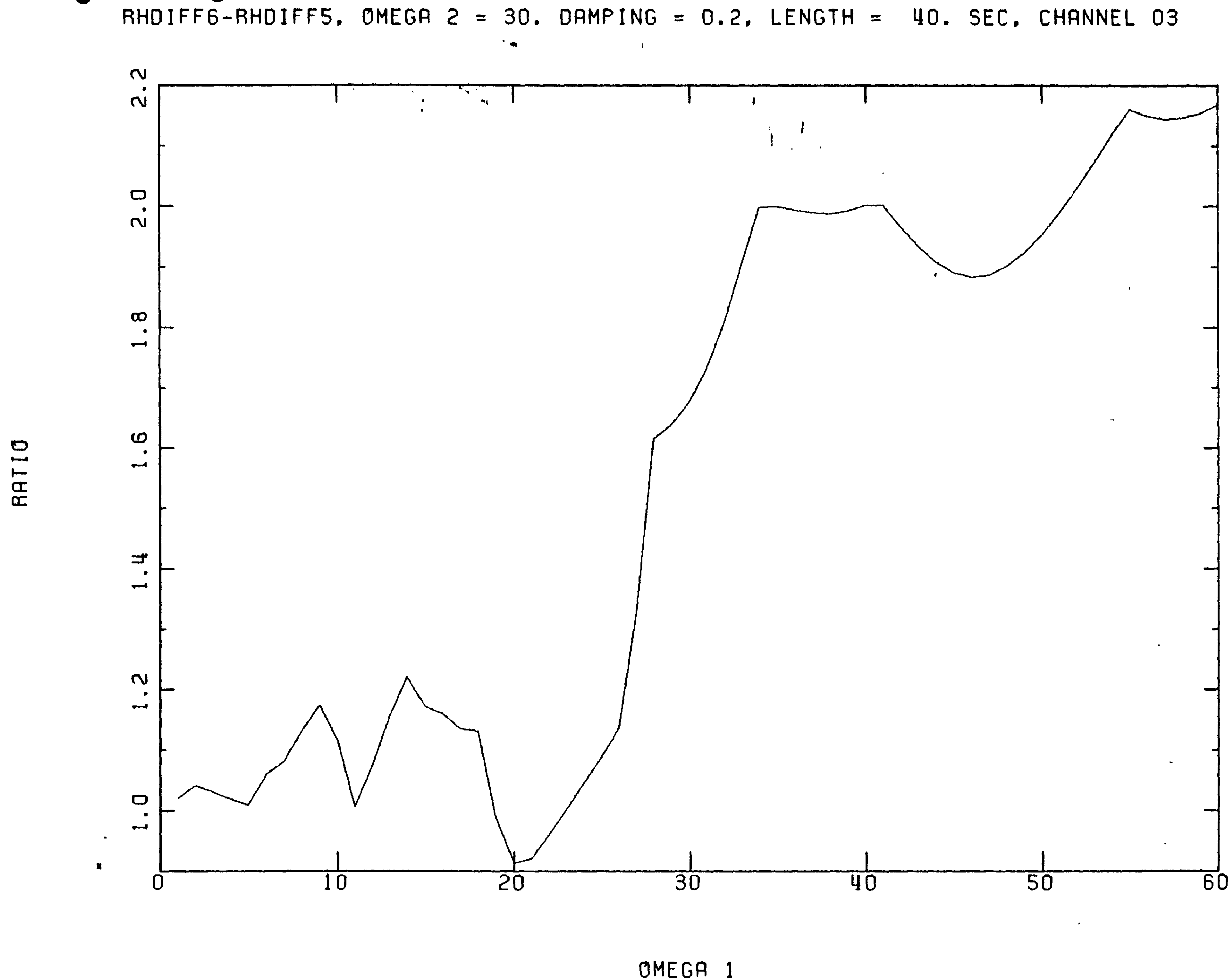
RHDIFF6-RHDIFF5, ØMEGA 2 = 30. DAMPING = 0.2, LENGTH = 40. SEC, CHANNEL 03
RATIØ
2.2
2.0
1.8
1.6
1.4
1.2
1.0
0
10
20
30
40
50
60
ØMEGA 1

Fig 24

RHDIFF5-RHDIFF1, ØMEGA 2 = ØMEGA 1 DAMPING = 0, LENGTH = 40. SEC, CHANNEL 03

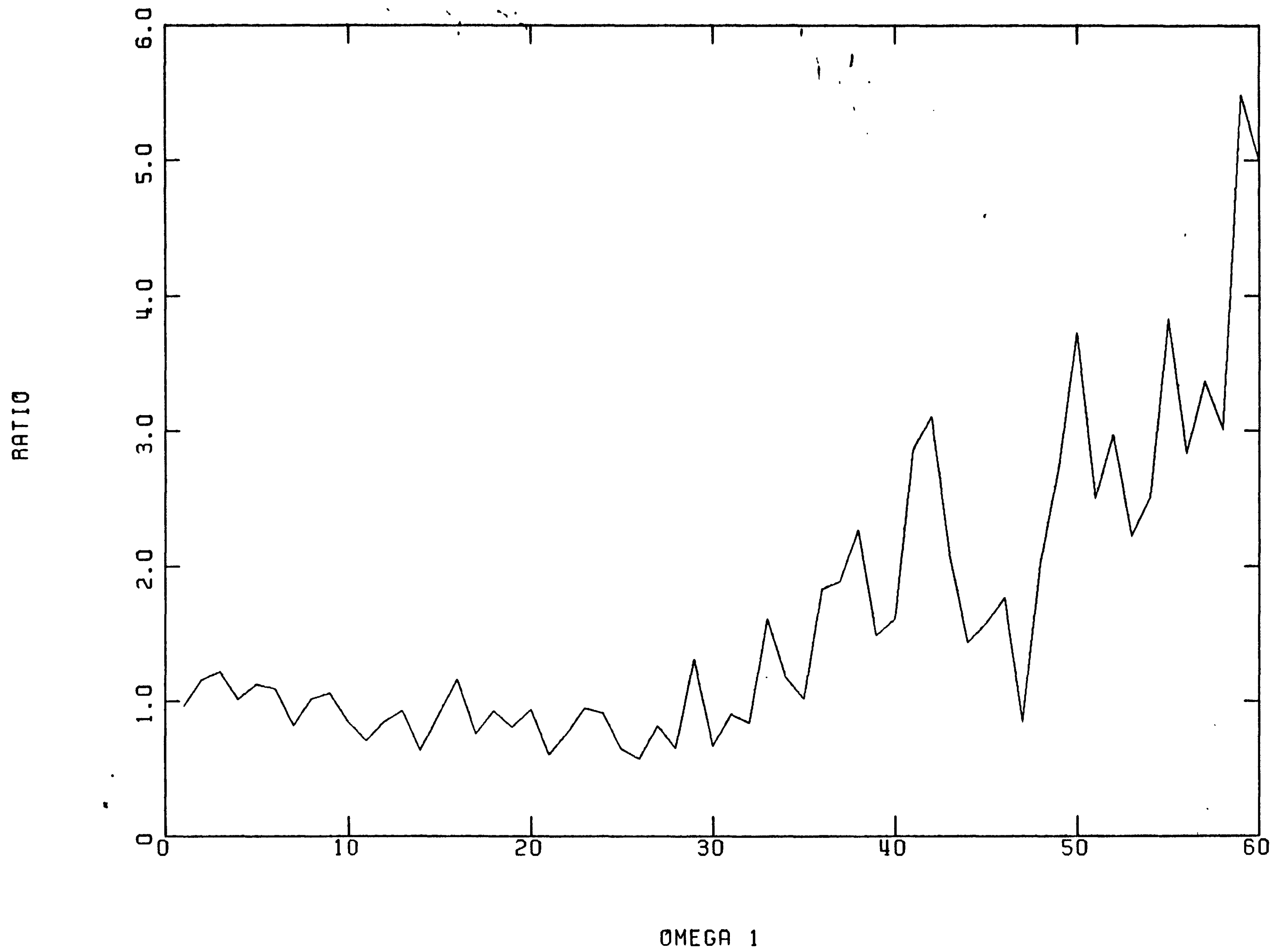

Fig 25

RHDIFF5-RHDIFF1, OMEGA 2 = OMEGA 1 DAMPING = 0.1, LENGTH = 40. SEC, CHANNEL 03

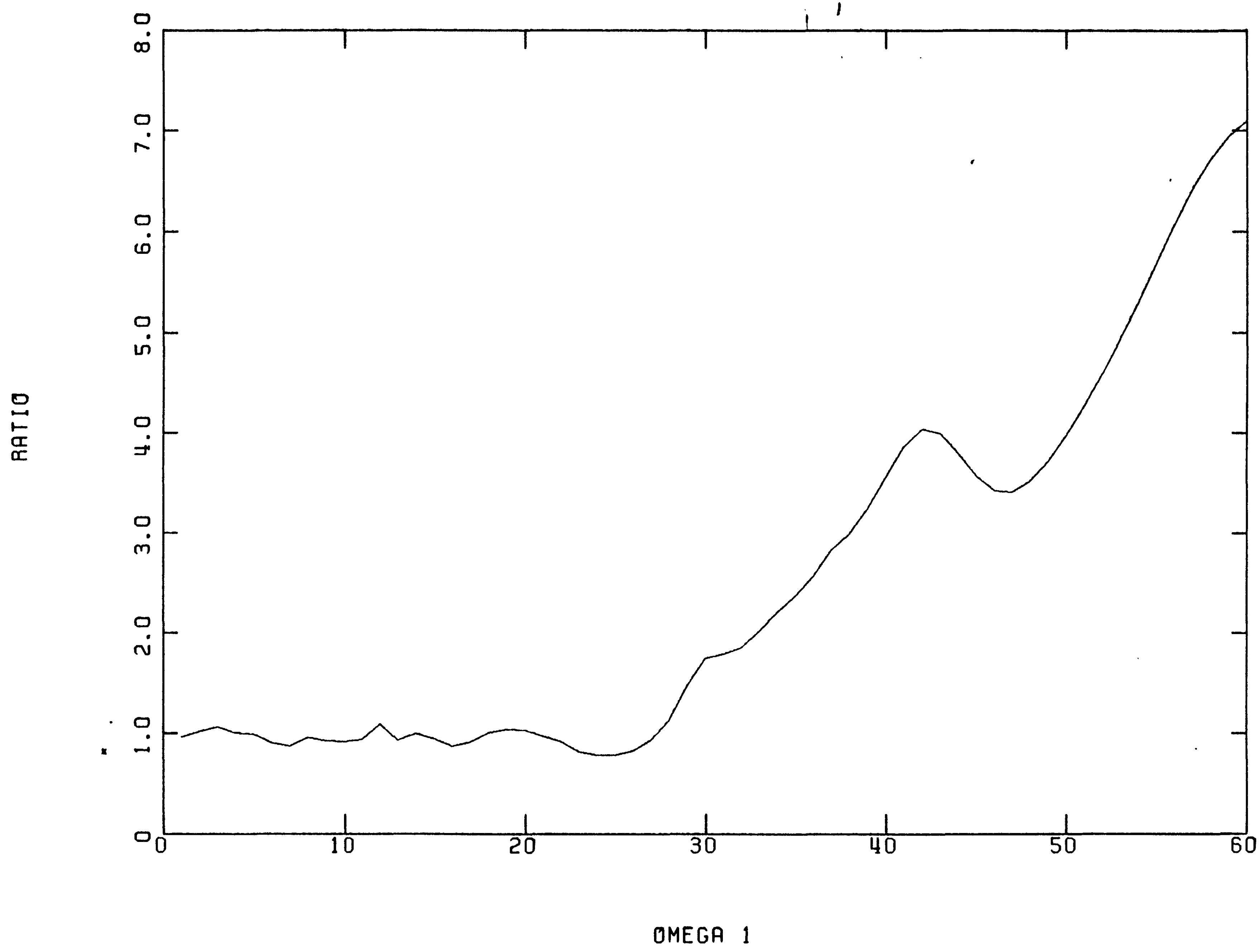

Fig 26

RHDIFF5-RHDIFF1, ØMEGA 2 = ØMEGA 1 DAMPING = 0.2, LENGTH = 40. SEC, CHANNEL 03

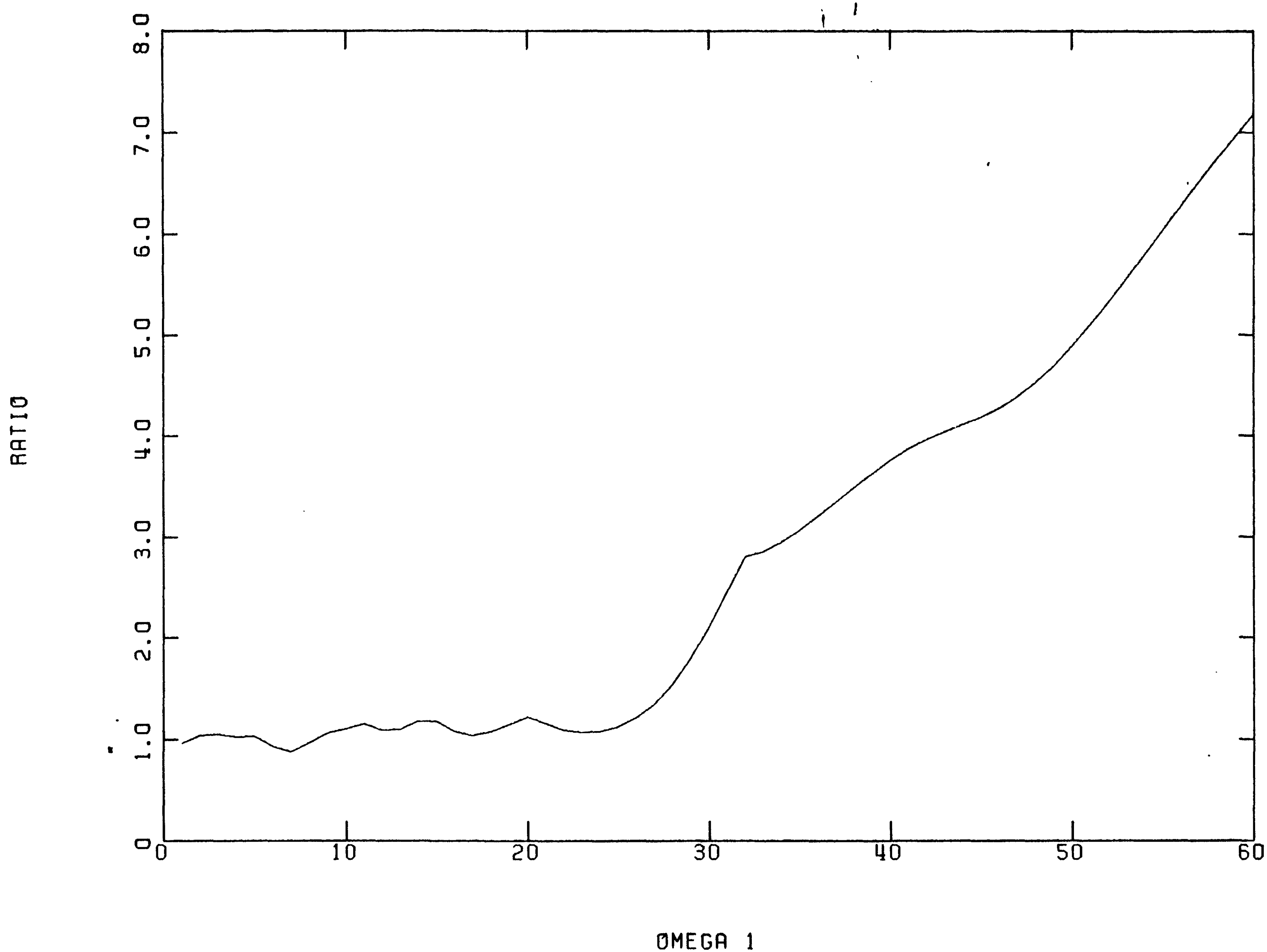

Fig 27

RHDIFF6-RHDIFF5, OMEGA 2 = OMEGA 1 DAMPING = 0.0, LENGTH = 40. SEC, CHANNEL 01

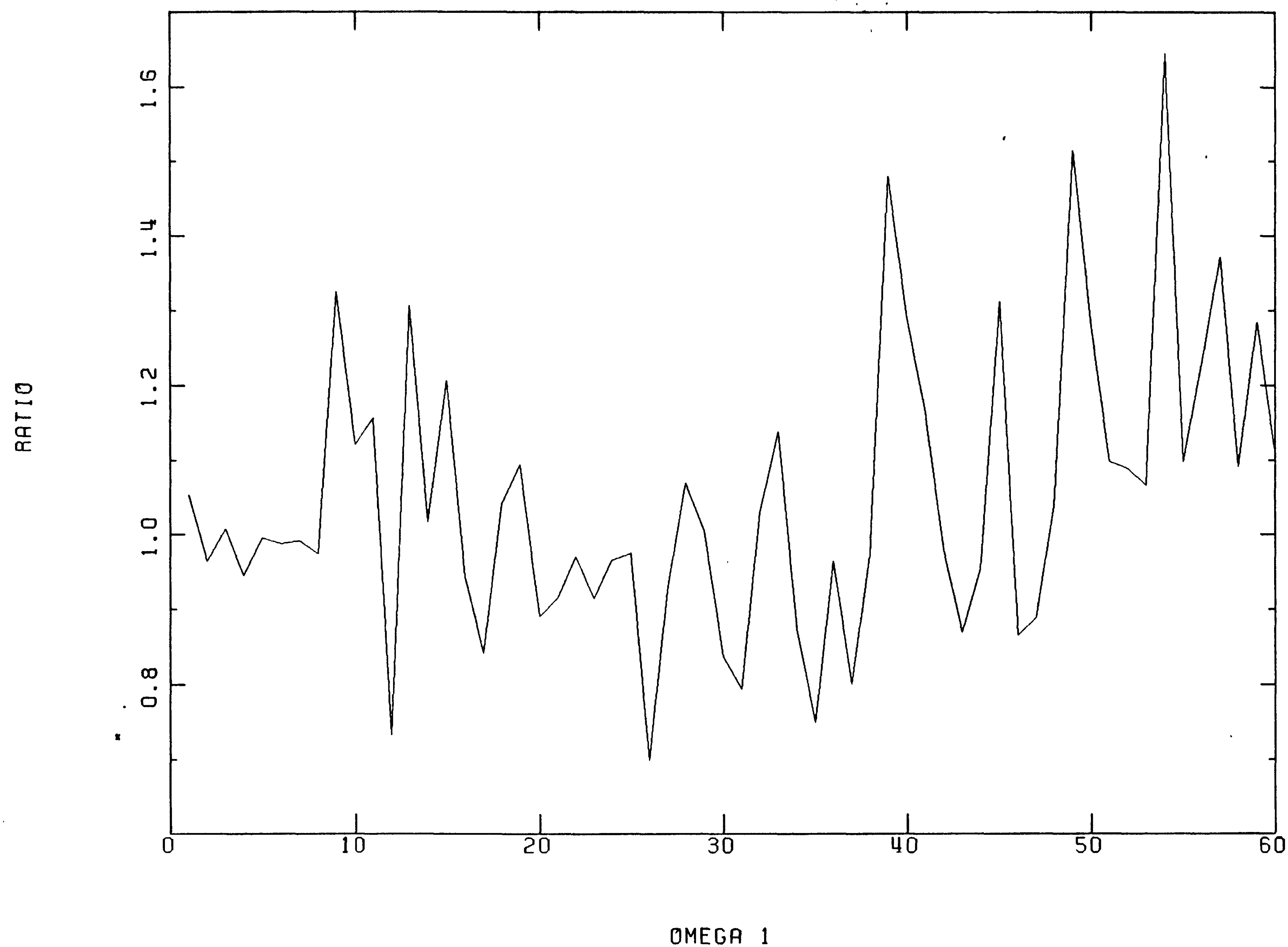

Fig 28

RHDIFF6-RHDIFF5, OMEGA 2 = 10. DAMPING = 0.0, LENGTH = 40. SEC, CHANNEL 01

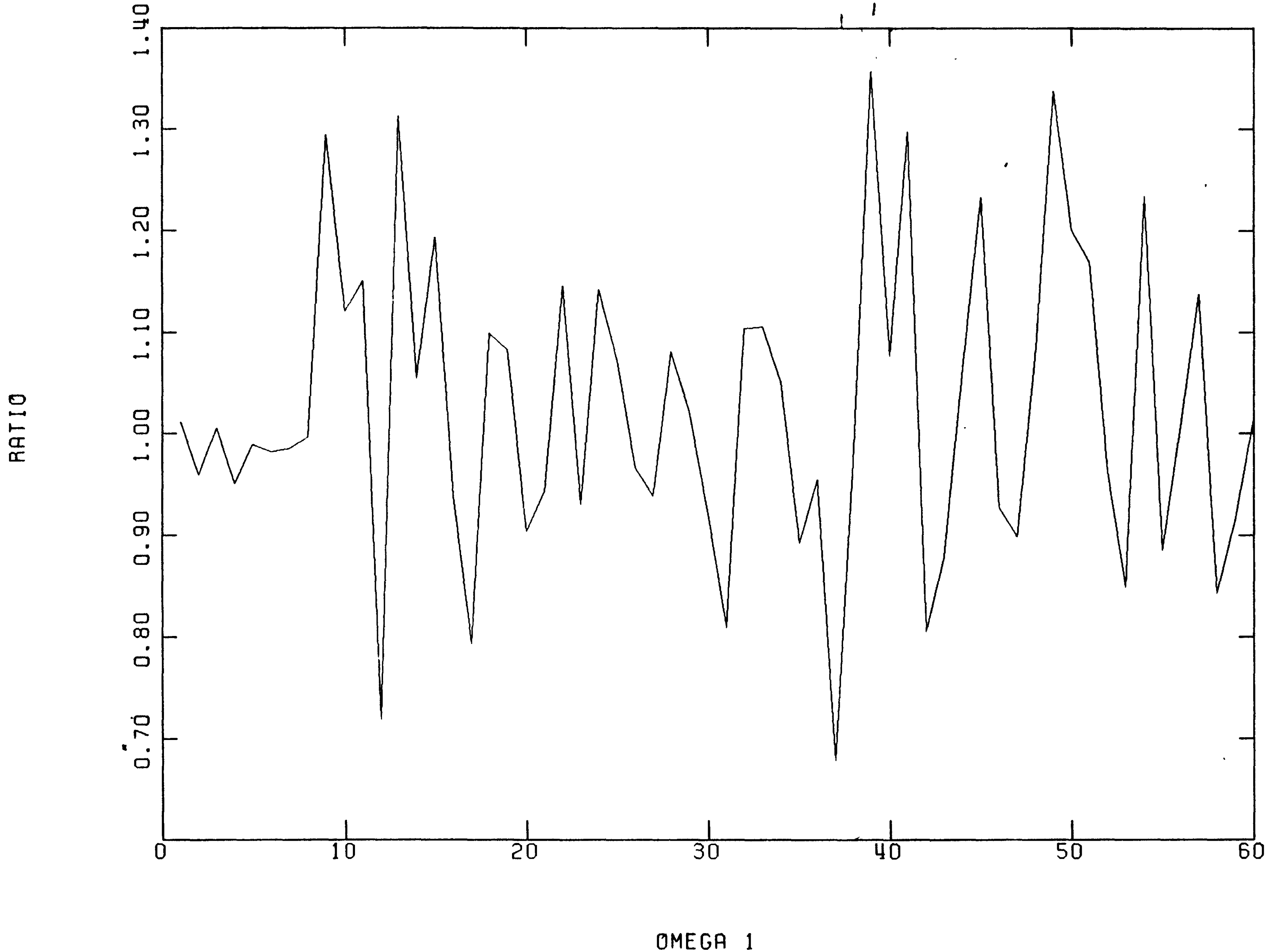

Fig 29

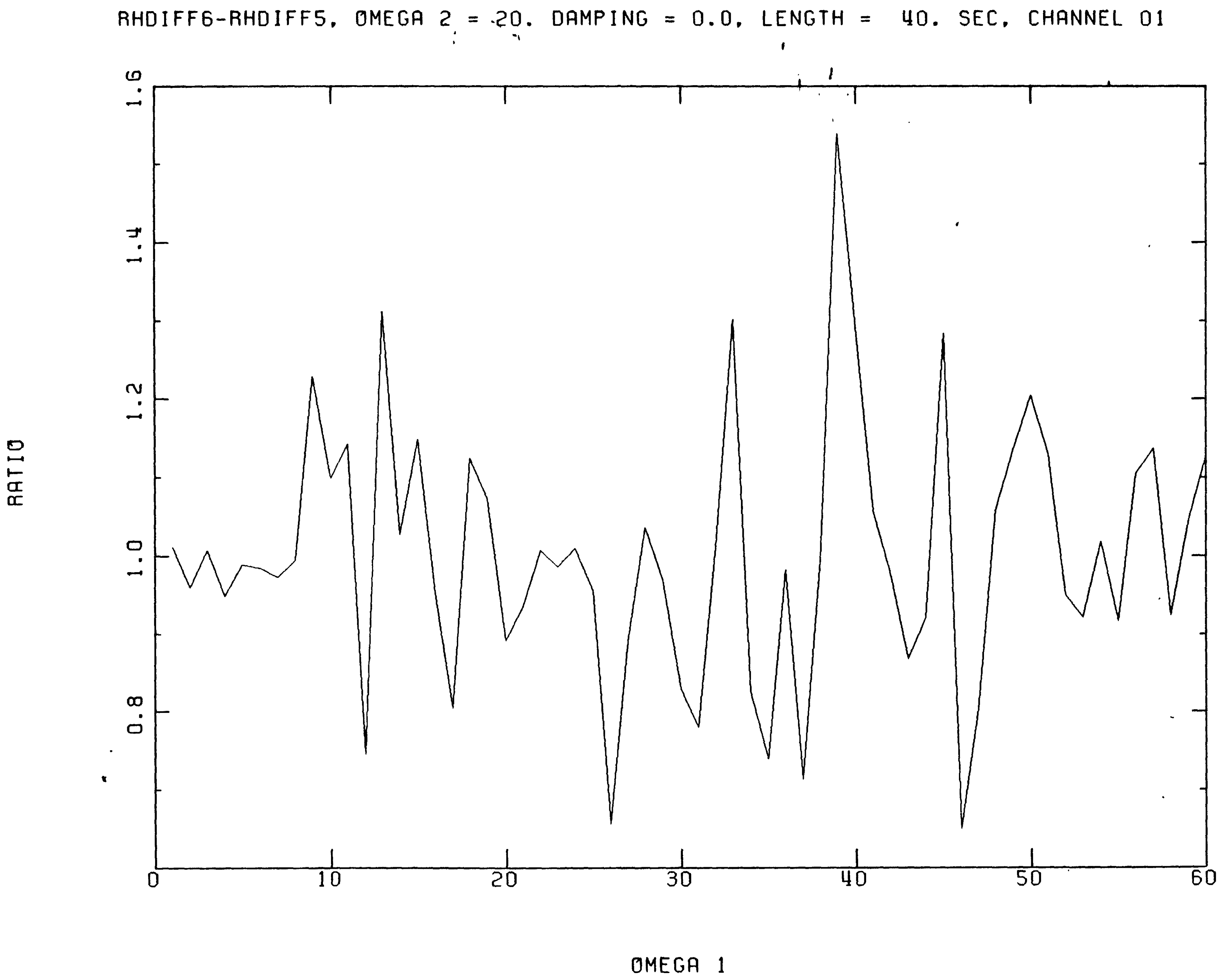

RHDIFF6-RHDIFF5, ØMEGA 2 = 20. DAMPING = 0.0, LENGTH = 40. SEC, CHANNEL 01
RATIO
1.6
1.4
1.2
1.0
0.8
0
10
20
30
40
50
60
ØMEGA 1

Fig 30

RHDIFF6-RHDIFF5, OMEGA 2 = 30, DAMPING = 0.0, LENGTH = 40. SEC, CHANNEL 01

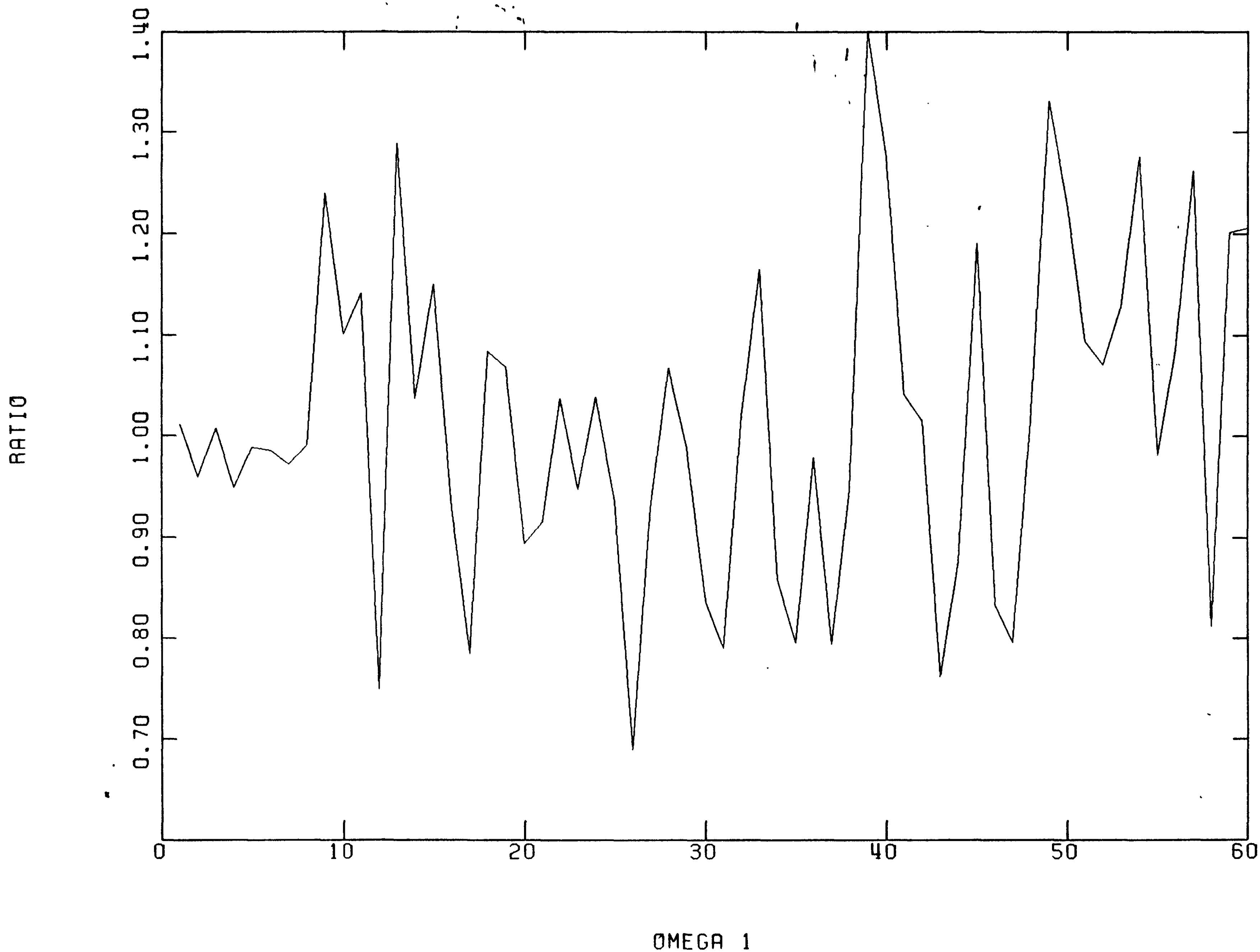

Fig 31

EL CENTRO DIFF ARRAY, TRANSVERSE (90 DEGREE) COMPONENT
NO. 3 MINUS NO. 1,NO. 2 MINUS NO. 1,NO. 3 MINUS NO. 2
WESTMORLAND EARTHQUAKE OF APRIL 1981
UNI BUTTERWORTH FILTER AT .167 HZ, ORDER 4

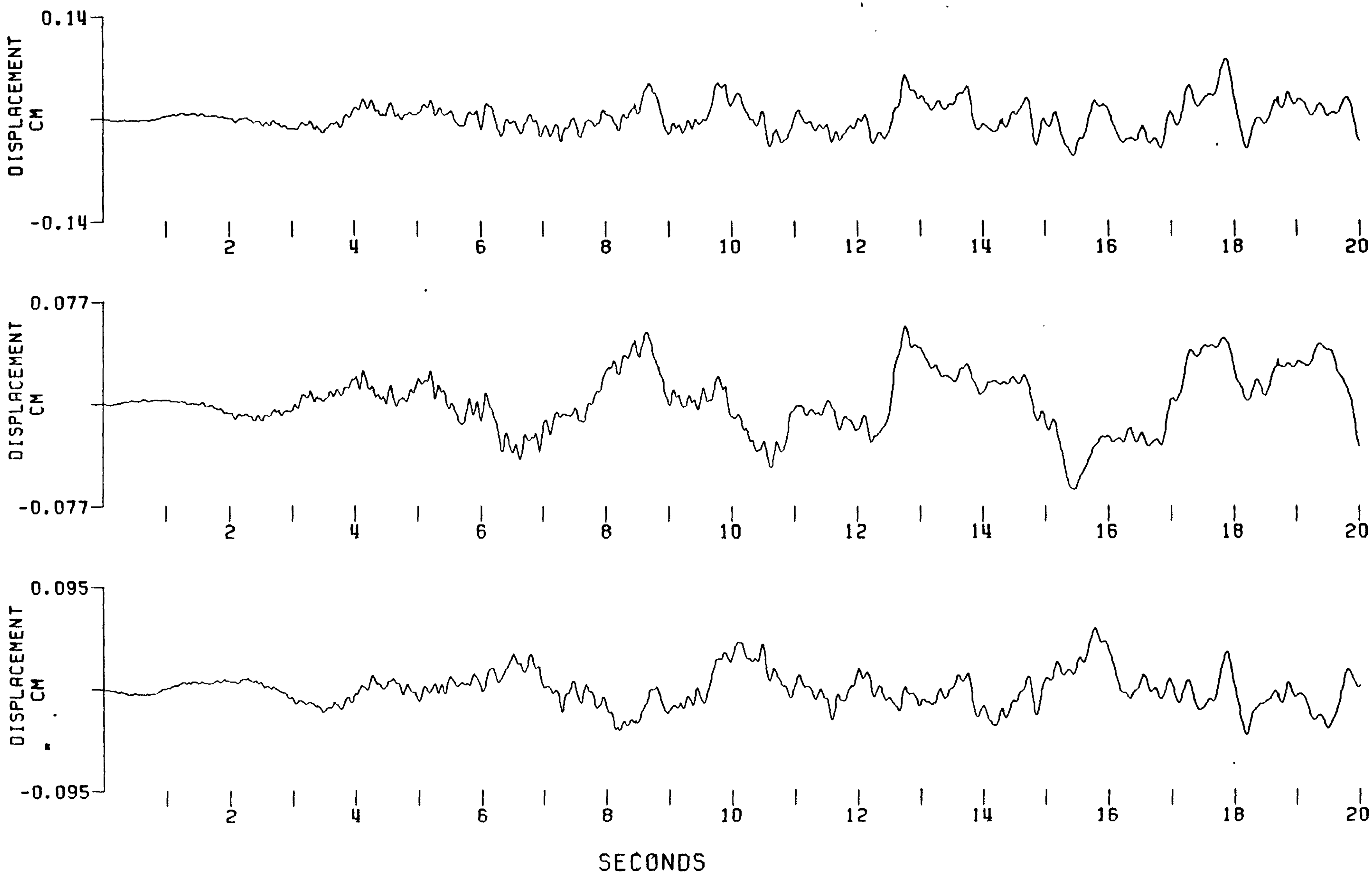

Fig 32

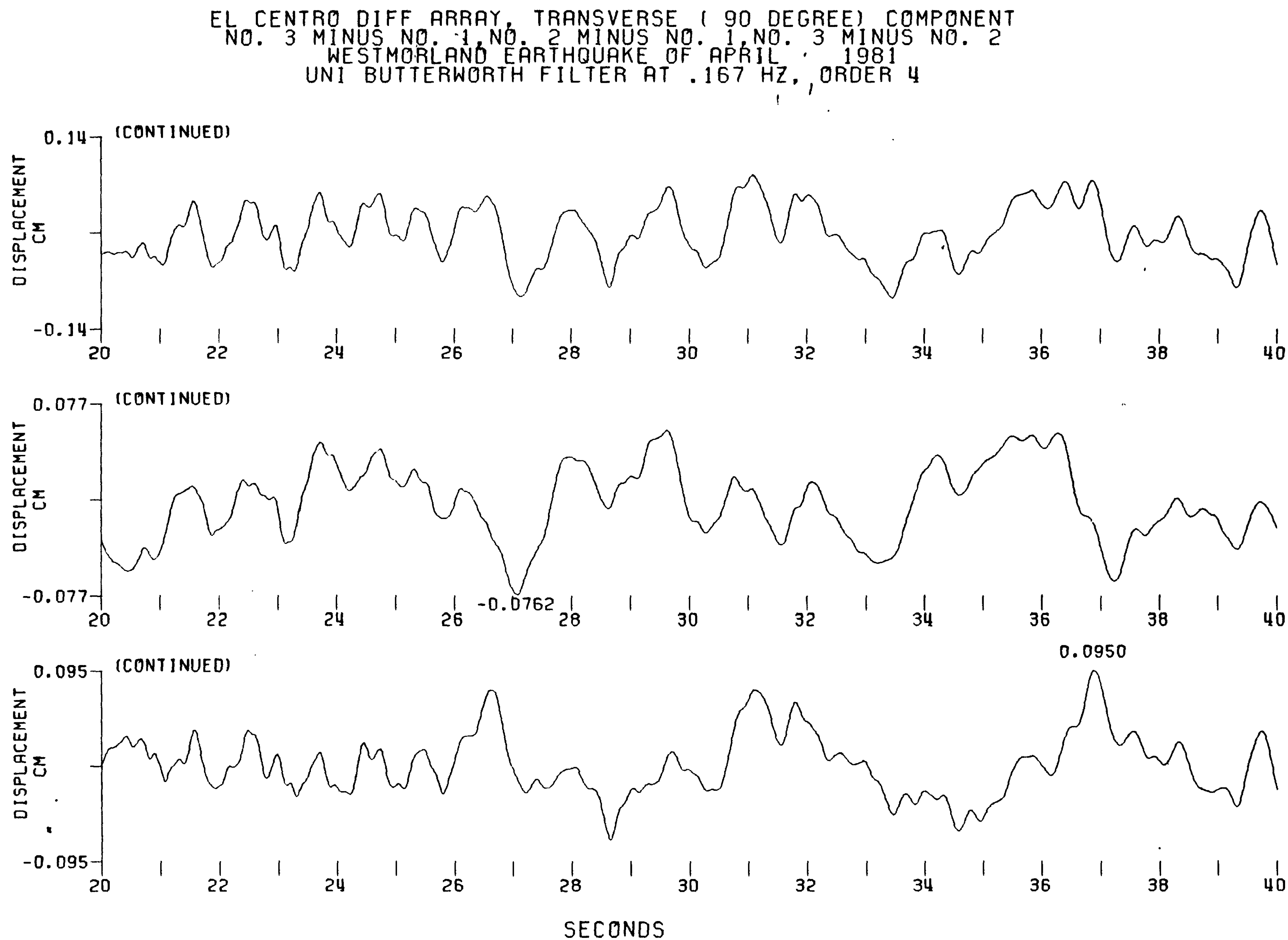
EL CENTRO DIFF ARRAY, TRANSVERSE (90 DEGREE) COMPONENT
NO. 3 MINUS NO. 1, NO. 2 MINUS NO. 1, NO. 3 MINUS NO. 2
WESTMORLAND EARTHQUAKE OF APRIL 1981
UNI BUTTERWORTH FILTER AT .167 HZ, ORDER 4
(CONTINUED)
0.14
-0.14
DISPLACEMENT CM
0.077
-0.077
-0.0762
0.095
-0.095
0.0950
20
22
24
26
28
30
32
34
36
38
40
SECONDS

Fig 33

EL CENTRO DIFF ARRAY, TRANSVERSE (90 DEGREE) COMPONENT
NO. 3 MINUS NO. 1, NO. 2 MINUS NO. 1, NO. 3 MINUS NO. 2
WESTMORLAND EARTHQUAKE OF APRIL 1981
UNI BUTTERWORTH FILTER AT .167 HZ, ORDER 4

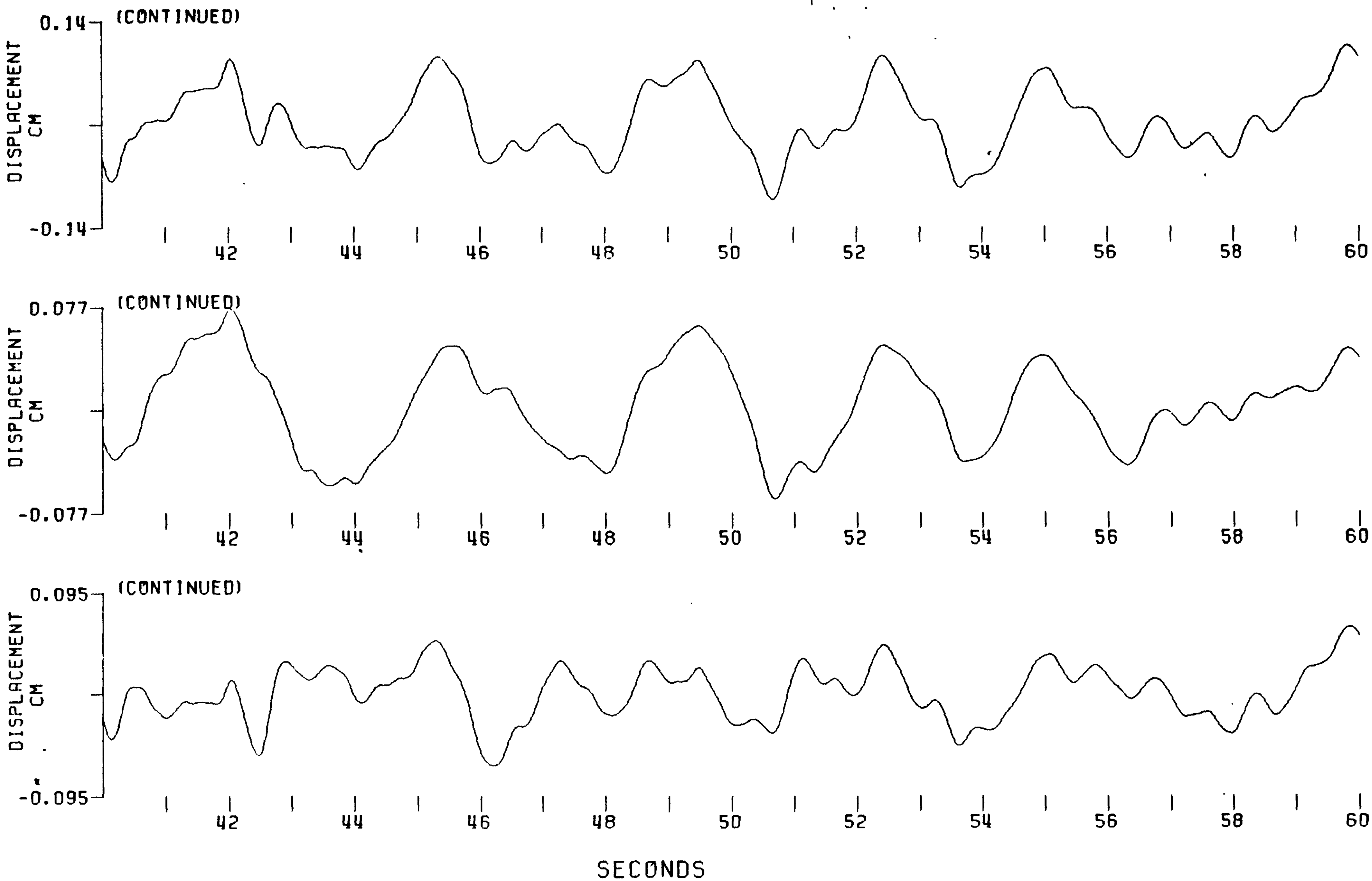

Fig 34

EL CENTRO DIFF ARRAY, LONGITUDINAL(180 DEGREE) COMPONENT
NO. 3 MINUS NO. 1,NO. 2 MINUS NO. 1,NO. 3 MINUS NO. 2
WESTMORLAND EARTHQUAKE OF APRIL 1981
UNI BUTTERWORTH FILTER AT .167 HZ, ORDER 4

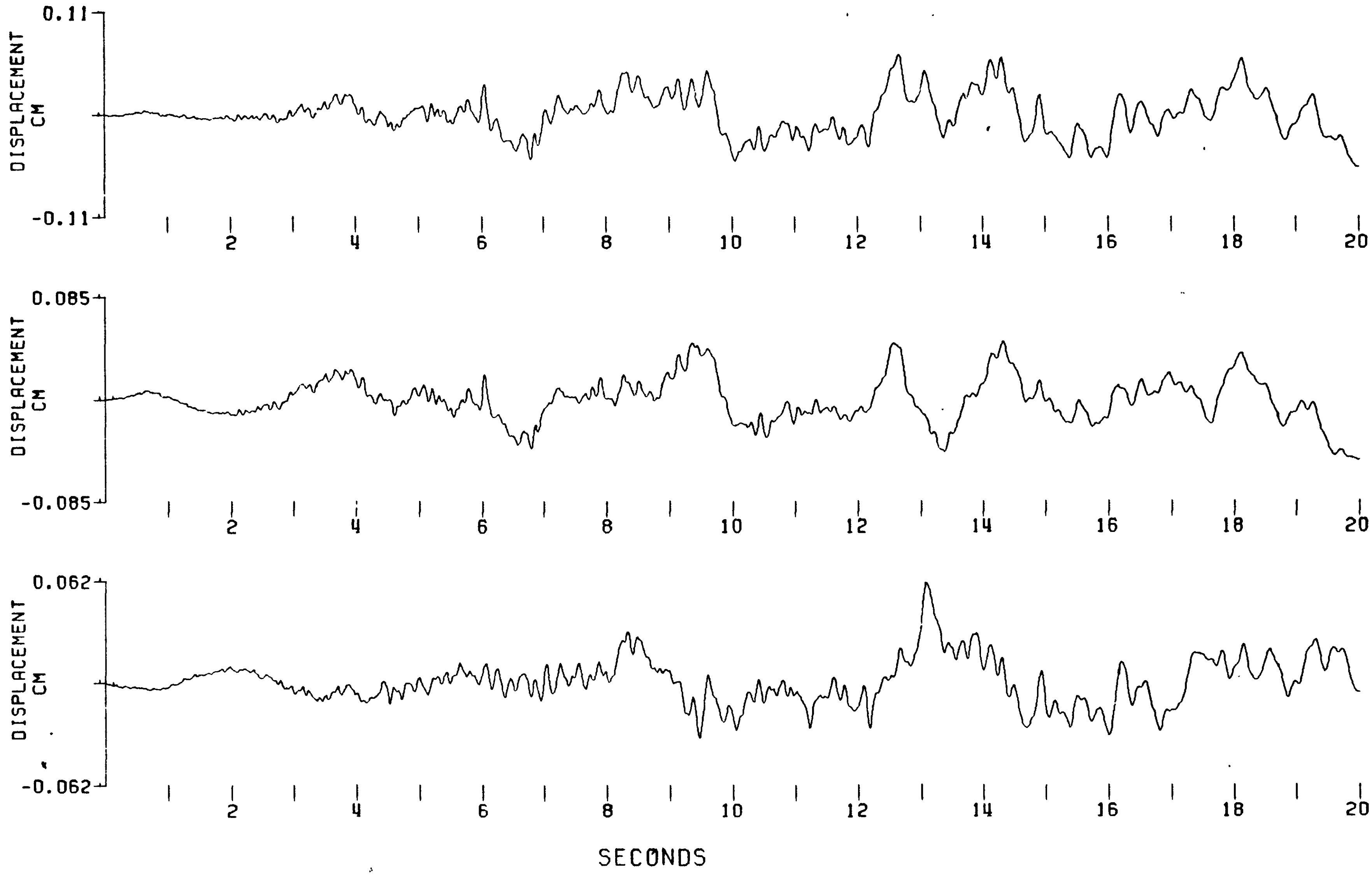

Fig 35

EL CENTRO DIFF ARRAY, LONGITUDINAL (180 DEGREE) COMPONENT
NO. 3 MINUS NO. 1, NO. 2 MINUS NO. 1, NO. 3 MINUS NO. 2
WESTMORLAND EARTHQUAKE OF APRIL 1981
UNI BUTTERWORTH FILTER AT .167 HZ, ORDER 4

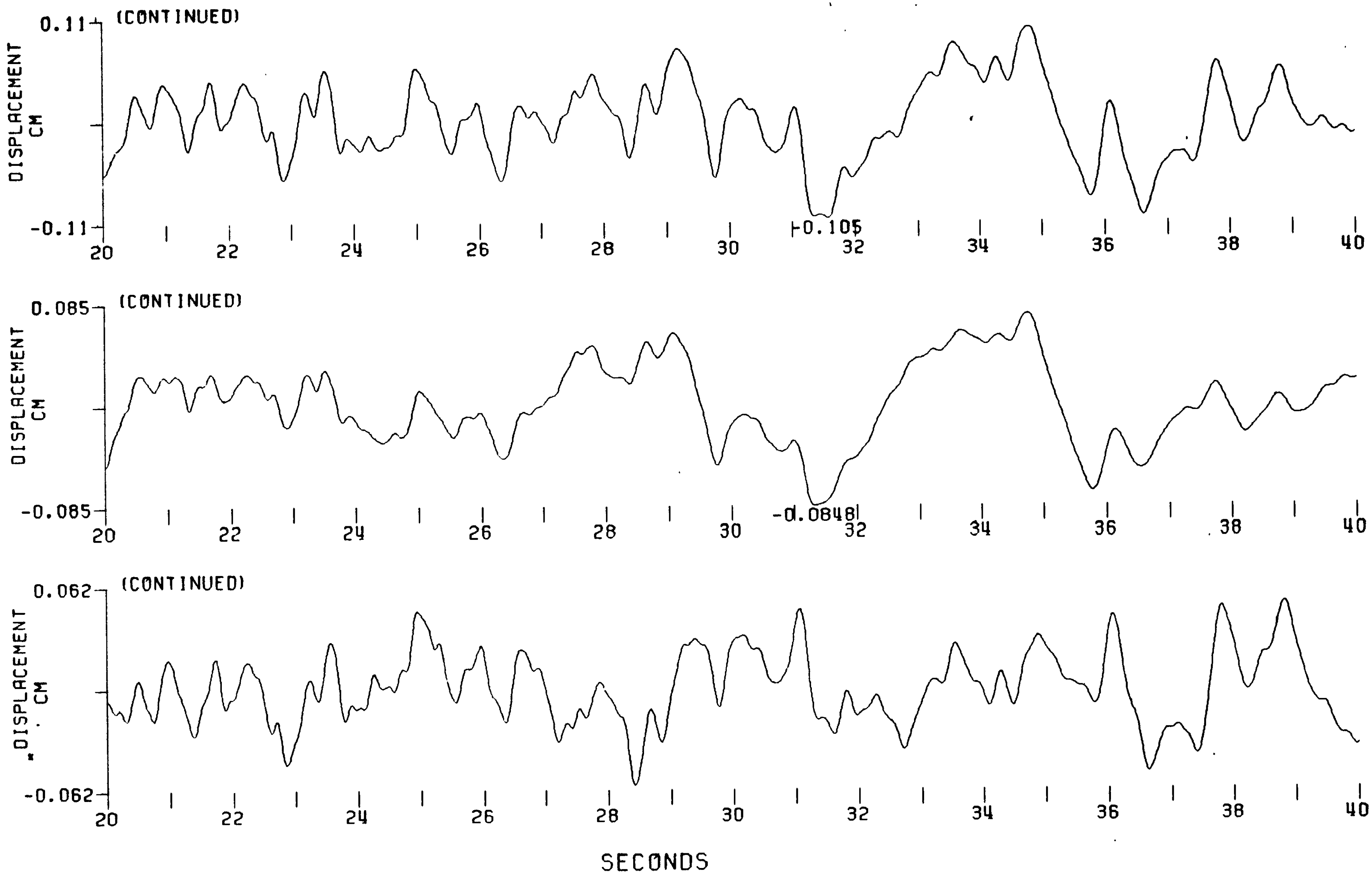

Fig 36

EL CENTRO DIFF ARRAY, LONGITUDINAL (180 DEGREE) COMPONENT
NO. 3 MINUS NO. 1, NO. 2 MINUS NO. 1, NO. 3 MINUS NO. 2
WESTMORLAND EARTHQUAKE OF APRIL , 1981
UNI BUTTERWORTH FILTER AT .167 HZ, ORDER 4

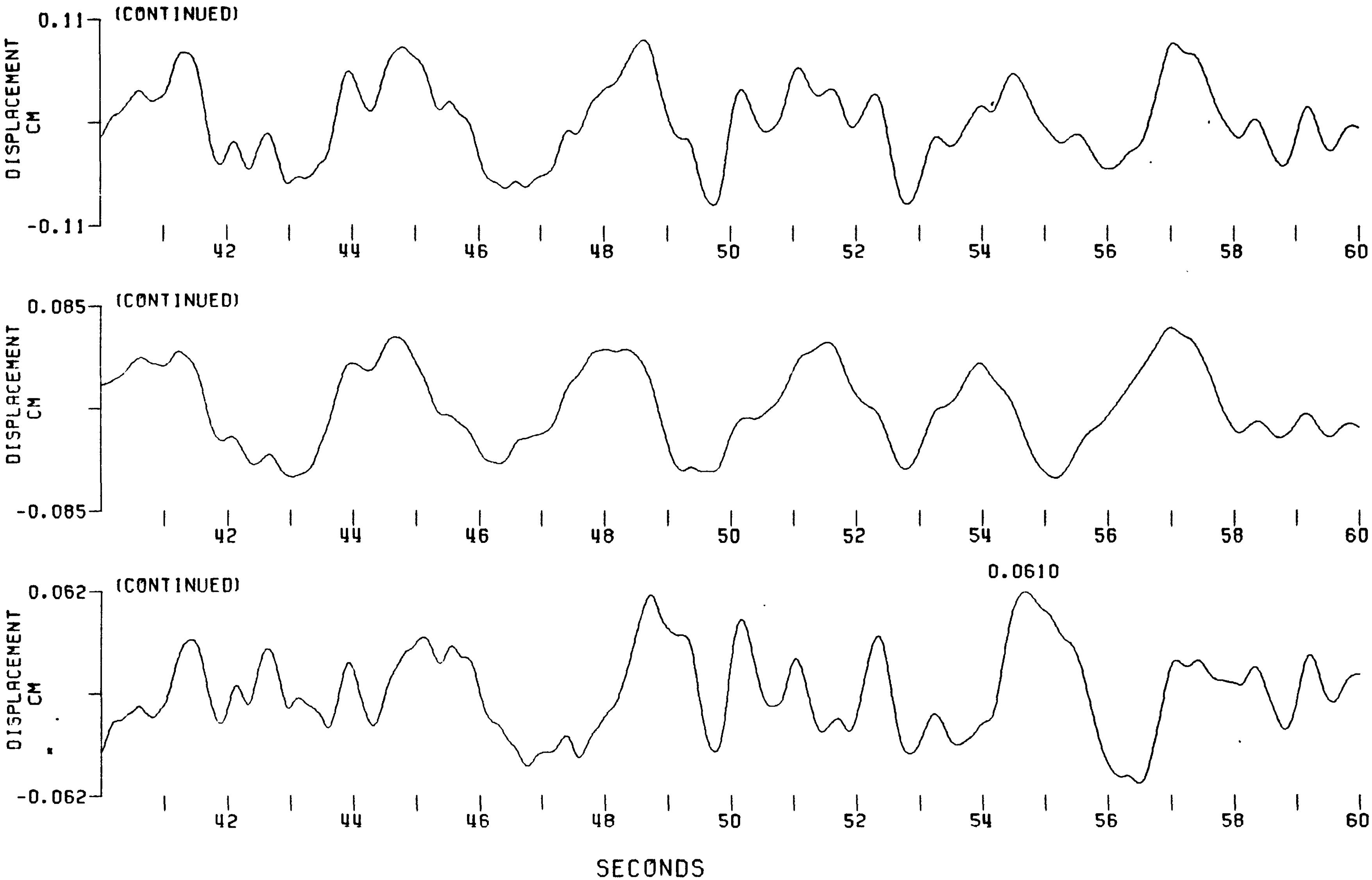

Fig 37

IV2WEST-IV1WEST, ØMEGA 2 = ØMEGA 1 DAMPING = 0, LENGTH = 60. SEC, CHANNEL 02

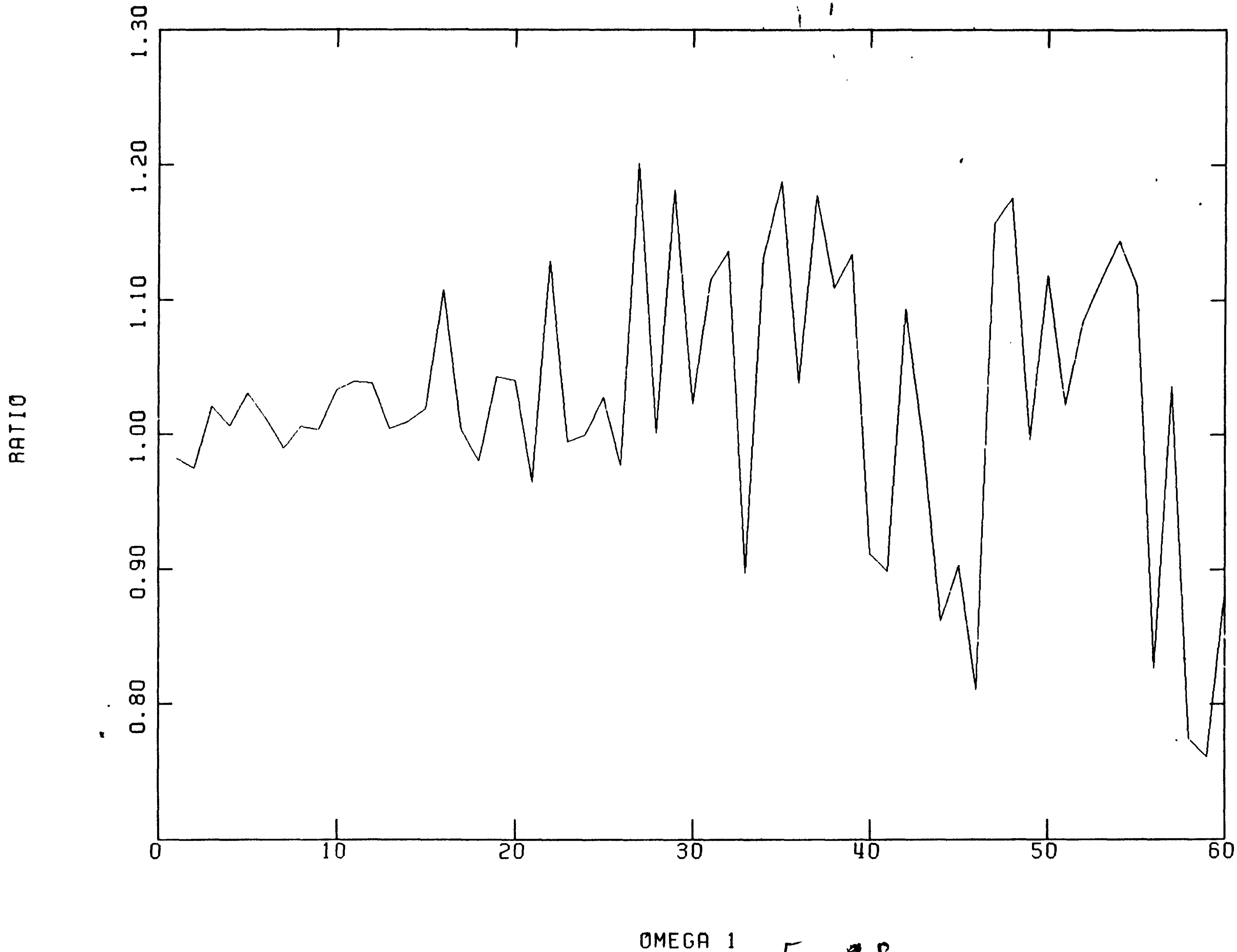

Fig 38

IV2WEST-IV1WEST, OMEGA 2 = OMEGA 1 DAMPING = 0.1, LENGTH = 60. SEC, CHANNEL 02

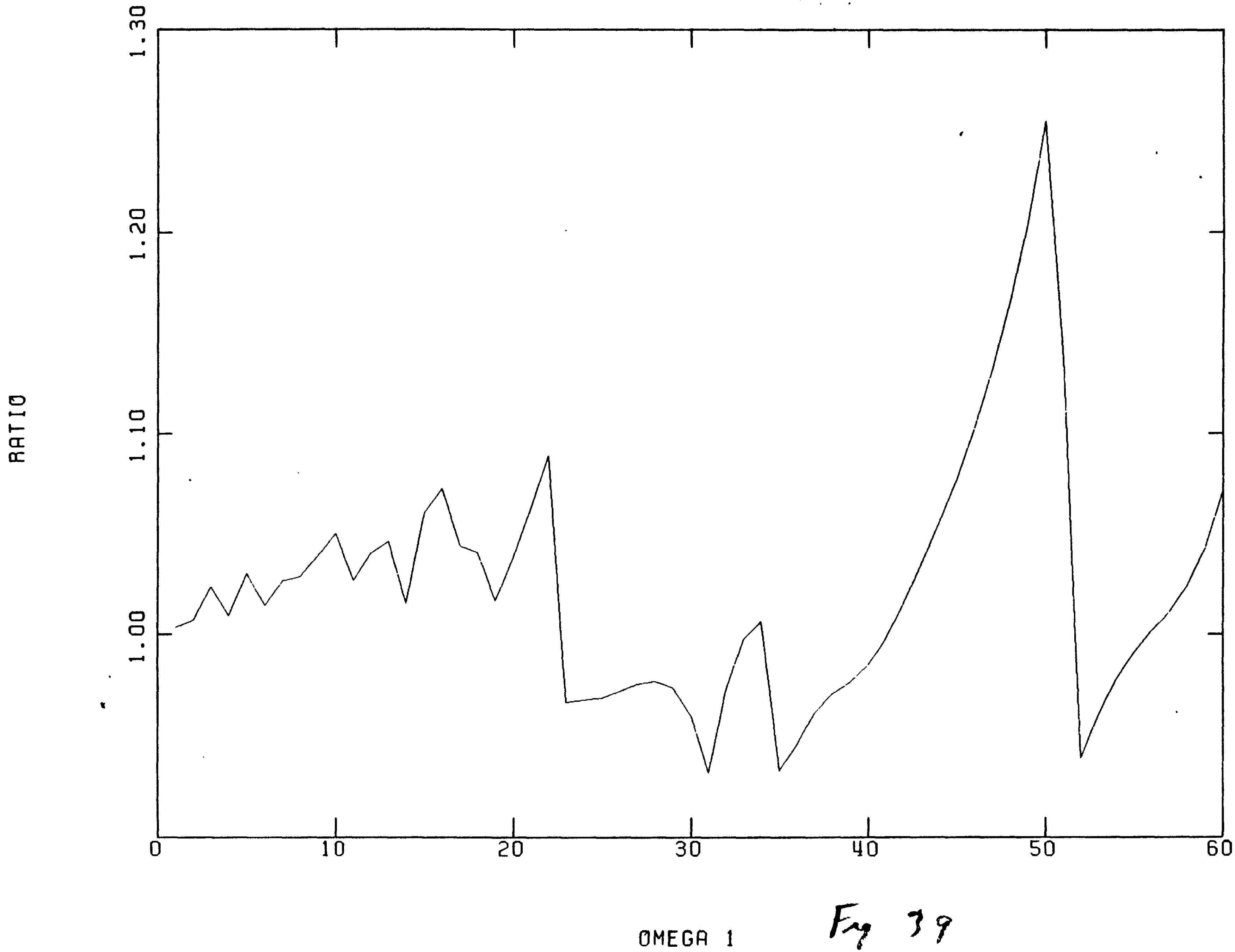

Fig 39

IV2WEST-IV1WEST, OMEGA 2 = OMEGA 1 DAMPING = 0.2, LENGTH = 60. SEC, CHANNEL 02

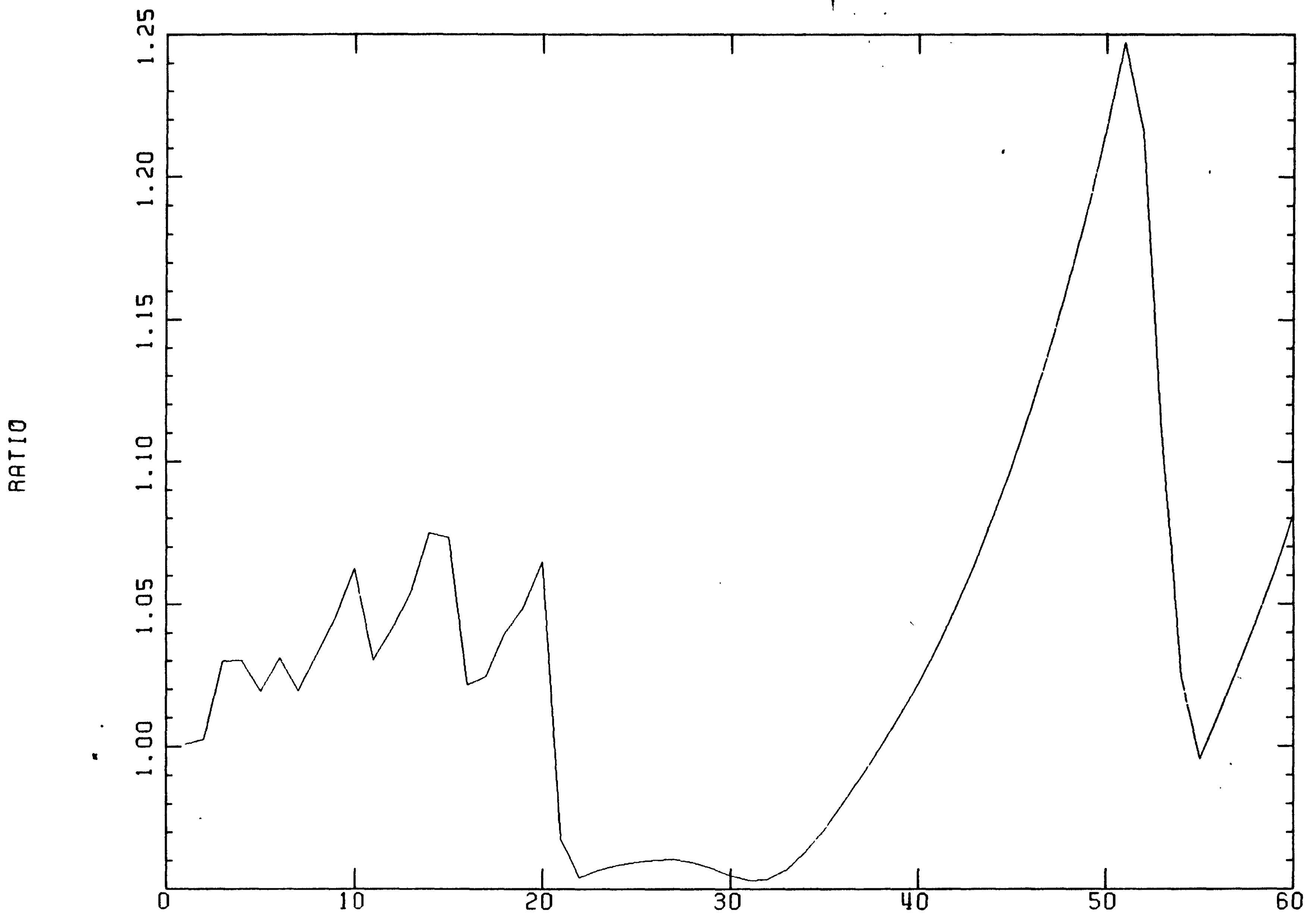

Fig 6 o

IV2WEST-IV1WEST, OMEGA 2 = 20.0 DAMPING = 0, LENGTH = 60. SEC, CHANNEL 02

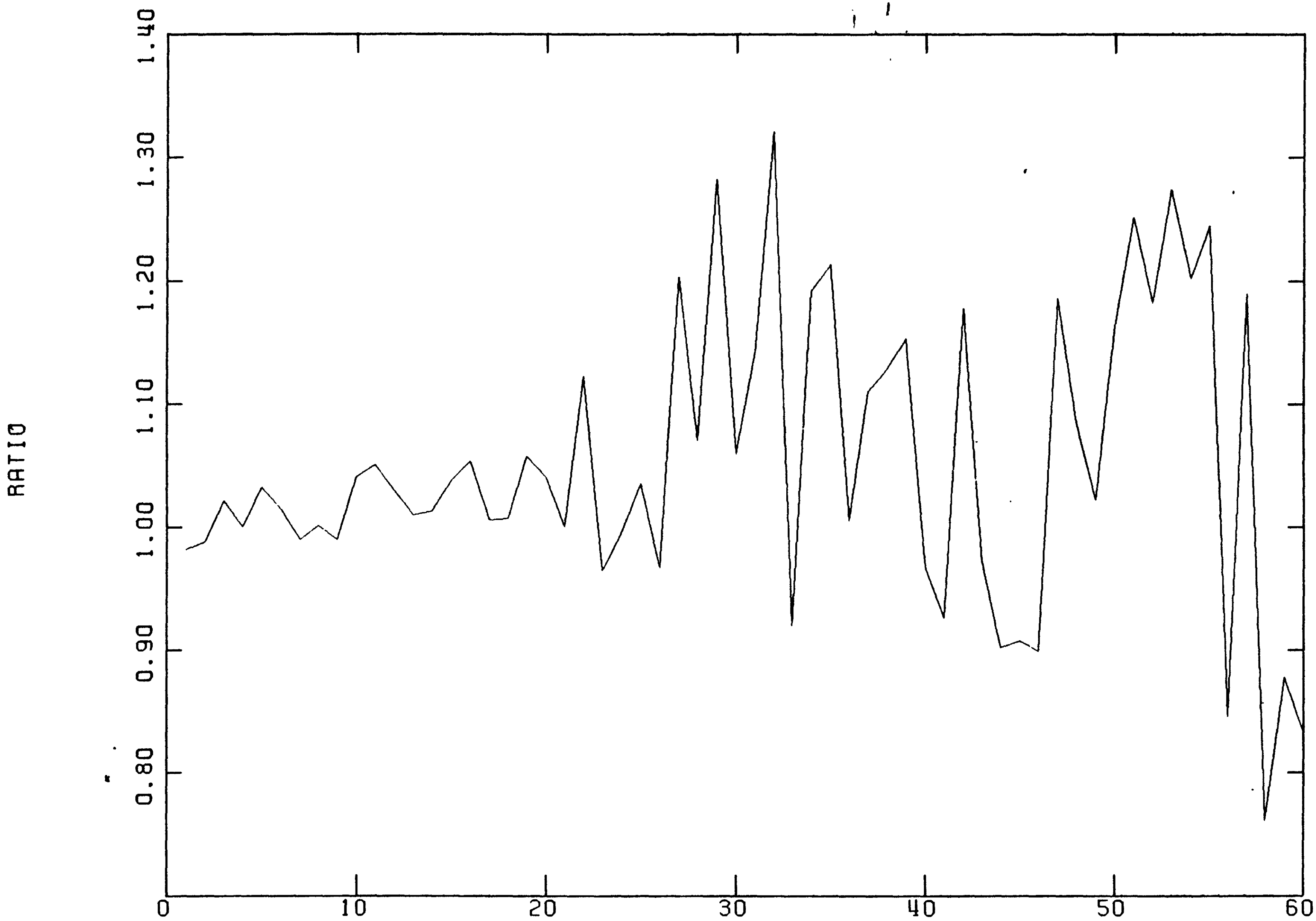

Fig 41

IV2WEST-IV1WEST, OMEGA 2 = 20.0 DAMPING = 0.1, LENGTH = 60. SEC, CHANNEL 02

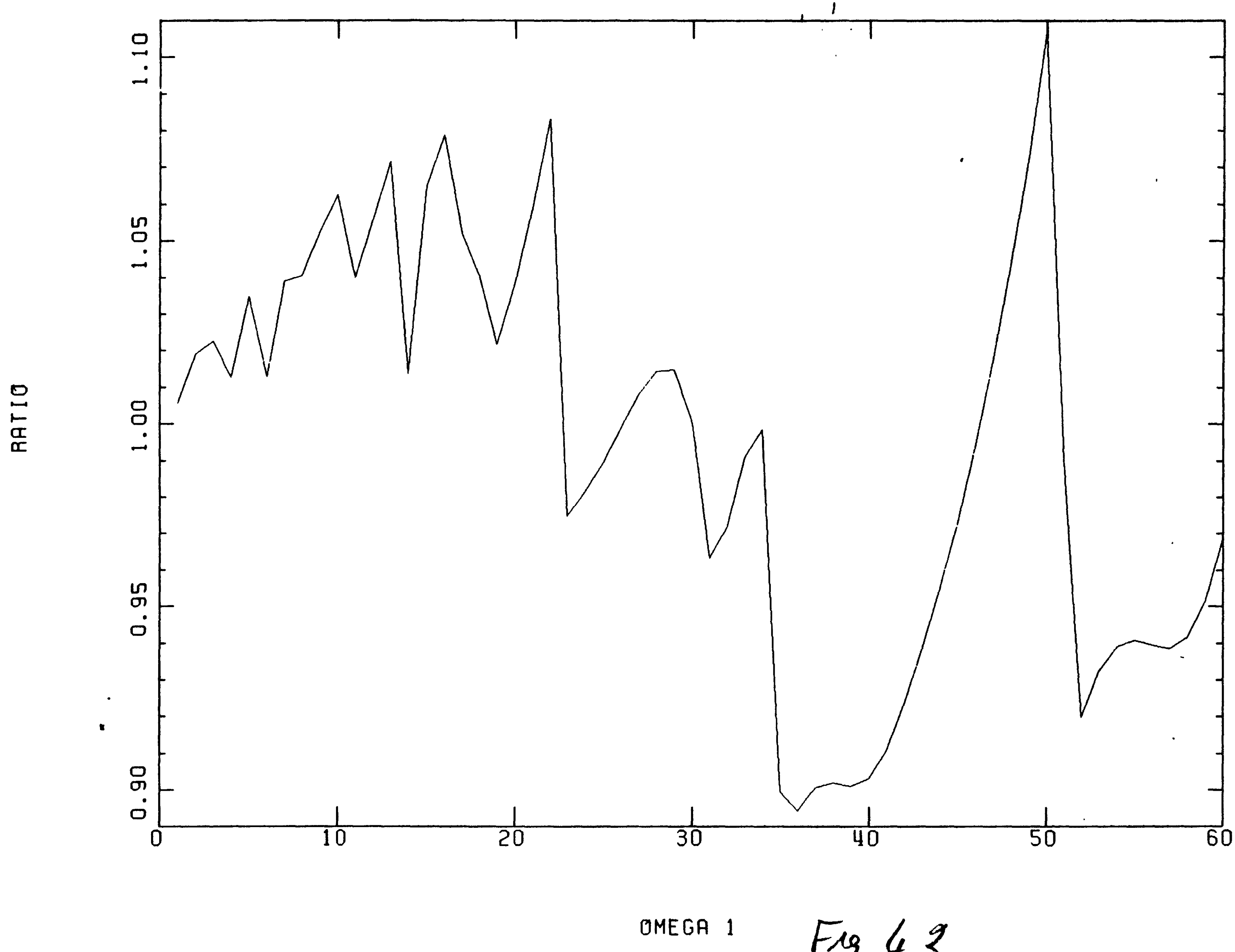

Fig 42

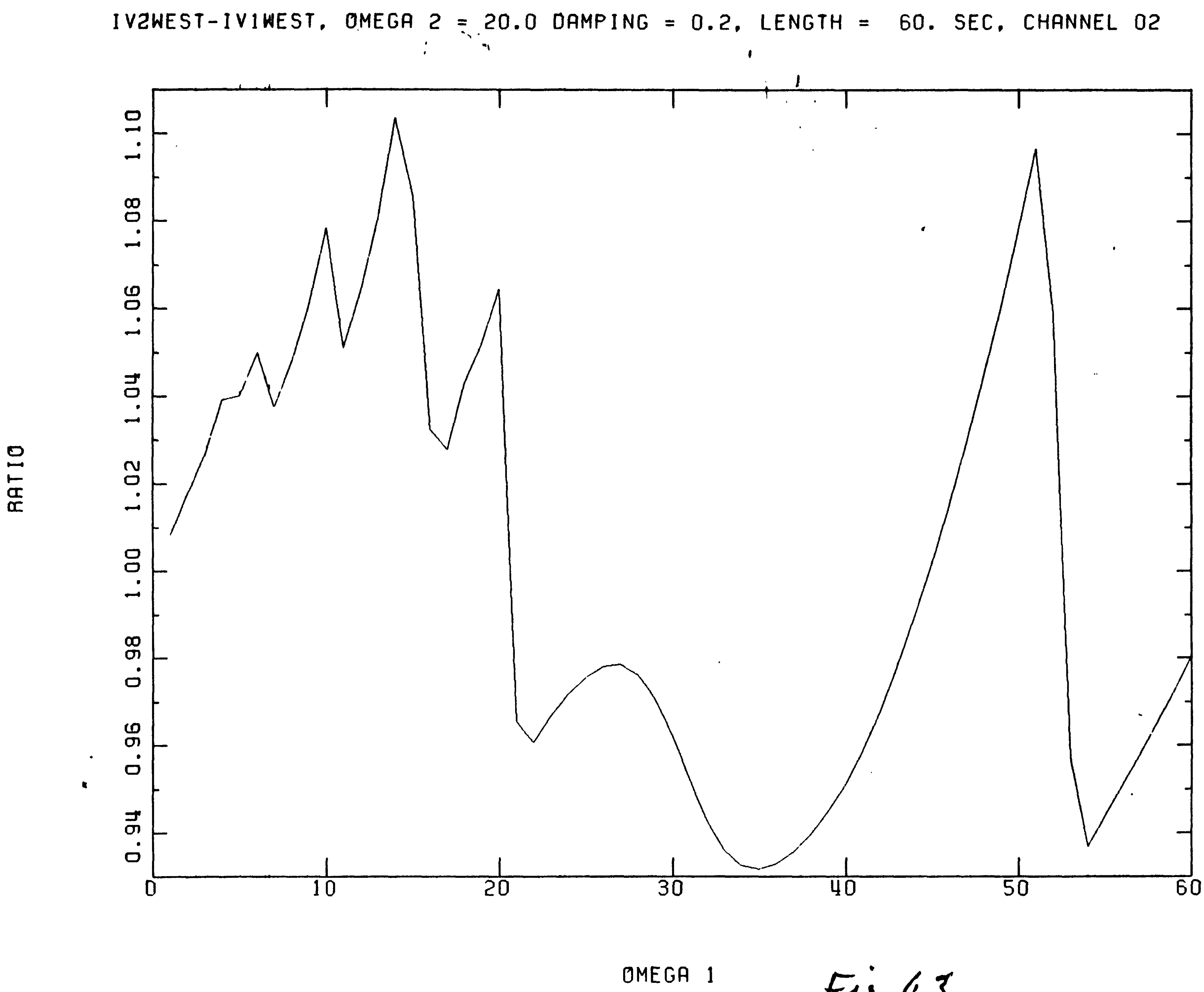
IV2WEST-IV1WEST, ØMEGA 2 = 20.0 DAMPING = 0.2, LENGTH = 60. SEC, CHANNEL 02
RATIO
1.10
1.08
1.06
1.04
1.02
1.00
0.98
0.96
0.94
0
10
20
30
40
50
60
ØMEGA 1

Fig 43